Modelling changes in secondary inorganic aerosol formation and nitrogen deposition in Europe from 2005 to 2030

Jan Eiof Jonson[1], Hilde Fagerli[1], Thomas Scheuschner[2], and Svetlana Tsyro[1]

[1]Norwegian Meteorological Institute, Oslo, Norway
[2]Umweltbundesamt, Dessau-Roßlau Germany

Correspondence: Jan Eiof Jonson (j.e.jonson@met.no)

Abstract.

Secondary inorganic $PM_{2.5}$ particles are formed from SO_x ($SO_2 + SO_4^{2-}$), NO_x ($NO + NO_2$), and NH_3 emissions, through the formation of either ammonium sulphate (($NH_4)_2SO_4$) or ammonium nitrate (NH_4NO_3). EU limits and WHO guidelines for $PM_{2.5}$ levels are frequently exceeded in Europe, in particular in the winter months. In addition the critical loads for eutrophication are exceeded in most of the European continent. Further reductions in NH_3 emissions and other PM precursors beyond the 2030 requirements could alleviate some of the health burden from fine particles, and also reduce the deposition of nitrogen to vulnerable ecosystems.

Using the regional scale EMEP/MSC-W model, we have studied the effects of year 2030 NH_3 emissions on $PM_{2.5}$ concentrations and depositions of nitrogen in Europe in the light of present (2017), past (2005), and future (2030) conditions. Our calculations show that in Europe the formation of $PM_{2.5}$ from NH_3 to a large extent is limited by the ratio between the emissions of NH_3 on one hand, and SO_x plus NO_x, on the other hand. As the ratio of NH_3 to SO_x and NO_x is increasing, the potential to further curb $PM_{2.5}$ levels through reductions in NH_3 emissions is decreasing. Here we show that per gram of NH_3 emissions mitigated, the resulting reductions in $PM_{2.5}$ levels simulated using 2030 emissions are about a factor of 2.6 lower than when 2005 emissions are used. However, this ratio is lower in winter. Thus further reductions in the NH_3 emissions in winter may have similar potentials as SO_x and NO_x in curbing $PM_{2.5}$ levels in this season.

Following the expected reductions of NH_3 emission, depositions of reduced nitrogen ($NH_3 + NH4^+$) should also decrease in Europe. However, as the reductions in NO_x emission are larger than for NH_3, the fraction of total nitrogen (reduced plus oxidised nitrogen) deposited as reduced nitrogen is increasing, and may exceed 60% in most of Europe by 2030. Thus the potential for future reductions in the exceedances of critical loads for eutrophication in Europe will mainly rely on the ability to reduce NH_3 emissions.

1 Introduction

Concentrations of particles with a diameter of less than 2.5 μm ($PM_{2.5}$) have been decreasing in most of Europe since the turn of the century as a combined result of reductions in anthropogenic emissions of primary particles and gaseous $PM_{2.5}$ precursors. Emissions of NH_3 play a central role in the secondary particle formation, and are also major contributors to the exceedances of critical loads for eutrophication (Tsyro et al., 2020). In most parts of Europe emissions of in particular SO_x (emitted predominantly as SO_2 but also as SO_4^{2-}), and NO_x ($NO + NO_2$), have been steadily decreasing in the past decades. At the same time, emissions of NH_3 have changed much less, decreasing in some European countries and increasing in others (see chapter 3 and appendix B in EMEP Status Report 1/2020 (2020)). Further reductions of SO_x, NO_x, and NH_3 emissions are required by the year 2030 according to the EU NEC2030 directive (https://www.eea.europa.eu/themes/air/air-pollution-sources-1/national-emission-ceilings), but the projected percentage reductions in NH_3 emissions in NEC2030 are smaller than for SO_x and NO_x. In the atmosphere SO_2 is oxidised to SO_4^{2-} and NO_x to HNO_3. Contrary to SO_x and NO_x, more than 90% of the NH_3 emissions are from agriculture, with only minor contributions from industry and traffic (IIASA, 2020). As a result these emissions are in general not co-located with the SO_x and NO_x emissions. In addition the temporal distribution of the emissions differ, with NH_3 emissions peaking in spring and summer, whereas anthropogenic SO_x and NO_x emissions in general peak in winter. In the fine mode, ammonium sulphate (($NH_4)_2SO_4$) particles are first formed from NH_3 and SO_4^{2-}. Any excess NH_3 can then form ammonium nitrate (NH_4NO_3) in thermodynamic equilibrium with HNO_3 (see e.g. Simpson et al. (2012)). When NH_3 is in excess relative to both SO_4^{2-} concentrations and the equilibrium with HNO_3, the formation of NH_4^+ salts will slow down at some point (when there is less acid available to react with NH_3), and free NH_3 (NH_3 in excess of SO_4^{2-}) will be present. With NH_3 emissions greatly exceeding SO_x and NO_x emissions already before 2005, one could question the effects of small or moderate reductions in NH_3 emissions on Secondary Inorganic Aerosols (SIA25), a major component in $PM_{2.5}$.

Using emissions as described in Jiang et al. (2020), Aksoyoglu et al. (2020) showed that the fraction of NH_4^+ in SIA25 was similar when calculated with 1990 versus 2030 emissions. With 1990 versus 2030 emissions the fraction of SO_4^{2-} in SIA25 dropped significantly, whereas the NO_3^- fraction increased, compensating for the reduction in SO_4^{2-}. In many air pollution episodes in Europe involving $PM_{2.5}$, NH_4NO_3 has accounted for a large portion of the aerosol mass (Petit et al., 2017; Vieno et al., 2016). With a large surplus of NH_3 relative to HNO_3 it could be that NH_4NO_3 formation will be virtually unaffected by changes in NH_3 emissions. Both NO_x and NH_3 are relatively shortlived, with a lifetime in the atmosphere of about 1 day (Seinfeld and Pandis, 2016). Given the difference in both spatial and temporal distribution in the sources of NH_3, NO_x, and SO_x, substantial local variability in the ratio between NH_3 on one hand, and SO_4^{2-} and/or HNO_3 on the other hand, can be expected. Thus, locally the formation of SIA25 may be limited by the availability of either NH_3 or by HNO_3 and SO_4^{2-} due to the lack of co-location in both space and time of the sources of these species.

Here we apply the EMEP MSC-W model to investigate how $PM_{2.5}$ concentrations, and deposition of reduced nitrogen ($NH_3 + NH_4^+$), have changed from 2005 to 2017. But the main focus is on model calculations for 2030, assuming that the NEC2030 requirements will be met. Given that NH_3 concentrations in Europe are generally in substantial excess of HNO_3

concentrations, we explore to what extent additional reductions in NH_3 emissions will contribute to further reductions in NH_4^+ and subsequently to reductions in $PM_{2.5}$ levels, and to what extent the response to further NH_3 emissions is linear. We try to answer this with a sensitivity study for $PM_{2.5}$ for post NEC2030, applying step-wise additional NH_3 emission reductions on top of the NEC2030 requirements holding all other emissions constant. At the same time we also investigate to what extent reductions in NH_3 emissions may affect deposition of reduced nitrogen and the exceedance of critical loads for nitrogen deposition.

2 Model description

The model calculations have been made with the EMEP MSC-W model (hereafter 'EMEP model'), version rv4.34, on 0.1 x 0.1° resolution for the domain between 30° W and 45° E and between 30 and 75° N. A detailed description of the EMEP model can be found in Simpson et al. (2012), with later model updates described in Simpson et al. (2020) and references therein. In the EMEP model the composition of the metastable aqueous aerosols of the inorganic system $NO_3^- - NH_4^+$ and water, and NH_3 – HNO_3 in the gas phase, are calculated using the MARS equilibrium model (Binkowski and Shankar, 1995). In Tsyro and Metzgert (2019) the EMEP model results using the MARS model are compared to model calculations with EQUSAM4clim (Metzger et al., 2016, 2018) giving very similar results.

The EMEP model is available as open source code (see code availability) and is under continuous development receiving feedback from a host of users. It is regularly evaluated against measurements, see Gauss et al. (2017, 2018, 2019, 2020) for the most recent evaluations. Scatter plots of model versus measurements for the concentrations of several key species, as well as for the wet depositions of reduced and oxidised nitrogen, are shown in appendix A. The model performance is comparable for both 2005 and 2017, even though the selection of measurement sites differs for the two years. Measurements are also available for subsets of common sites for the two years, in general showing comparable model to measurement biases for the concentrations of key species for the years 2005 and 2017. The EMEP model has also participated in model intercomparisons and model evaluations in a number of peer reviewed publications (Karl et al., 2019; Colette et al., 2011, 2012; Jonson et al., 2018). In Vivanco et al. (2018) depositions of sulphur and nitrogen species in Europe have been calculated by 14 regional models and compared to measurements, and in Theobald et al. (2019) the model calculated trends in the wet deposition of SO_4^{2-} as well as reduced and oxidised nitrogen from 6 models, including the EMEP model, are compared to measurements from 1990 to 2010. These two studies showed good results for the EMEP model. Out of the 14 models included in the study by Vivanco et al. (2018), the EMEP model was one of very few with low fractional biases compared to measurements for the wet depositions of reduced nitrogen (-0.01), oxidised nitrogen (-0.05), and SO_4^{2-} (-0.11). For the trend studies presented in Theobald et al. (2019) the fractional bias for the years 1990 to 2010 was -0.18, -0.02, and 0.22 for the wet deposition of reduced nitrogen, oxidised nitrogen, and SO_4^{2-} respectively, but the overall overestimation of SO_4^{2-} was mainly caused by an overestimation in the first years of the period. Running the EMEP model in global mode Ge et al. (2021) showed that the model captures the overall spatial and seasonal variations well for the major inorganic pollutants NH_3, NO_2, SO_2, HNO_3, NH_4^+, NO_3^-, and SO_4^{2-}, and wet depositions in East Asia, Southeast Asia, Europe, and North America.

2.1 Definition of the Critical Load for eutrophication

90 A Critical Load (CL) is defined as "a quantitative estimate of an exposure to one or more pollutants below which significant harmful effects on specified sensitive elements of the environment do not occur according to present knowledge" (Nilsson and Grennfelt, 1988). CLs are calculated for different receptors (e.g. terrestrial ecosystems, aquatic ecosystems), and a sensitive element can be any part (or the whole) of an ecosystem or ecosystem process. CLs have been derived for several pollutants and different negative effects. Here we restrict ourselves to CL defined to avoid the eutrophying effects of Nitrogen deposition

95 (CLeutN). Like sulphur, nitrogen can also have acidifying impacts in ecosystems, but the areas affected by acidification are strongly decreasing in Europe compared to earlier decades, and therefore the focus of this paper is on the eutrophying effects (Slootweg et al., 2015; EEA, 2014; Hettelingh et al., 2017).

The CLeutN for a site is either empirically derived or calculated from steady-state simple mass balance (SMB) equations. In the SMB method, non-harmful nitrogen-fixing processes are described mathematically and combined with a chemical criterion

100 (e.g., an acceptable N concentration in the soil solution). This summation is then compared to the corresponding deposition value. Methods to compute CLs are summarised in the Mapping Manual of the ICP Modelling and Mapping CLRTAP (2017), (see also De Vries et al. (2015)), which is used within the Convention on Long-range Transboundary Air Pollution: https://unece.org/40-years-clean-air.

If the deposition of the pollutant under consideration is greater than the CL at a site, the CL is designated as exceeded.

105 Such site-specific exceedances can be summarised for different spatial entities (e.g. grid cells, countries). This method is called average accumulated exceedance, and is defined as the weighted average of exceedances for all ecosystems within the selected region, where the weights are the respective ecosystem areas (Posch et al., 2001).

The CL exceedances presented here were calculated using the current CL database, which is described in Hettelingh et al. (2017) and stored by the current Coordination Centre for Effects (CCE) at the German Federal Environmental Agency. The

110 calculation is based on an extensive set of input data and equations. A detailed description is included in the Mapping Manual of the ICP Modelling and Mapping. (CLRTAP (2017), Chapter 5). This dataset is also used, among other things, to support European assessments and negotiations on emission reductions (Hettelingh et al., 2001; Reis et al., 2012; EEA, 2014).

3 Model runs

The EMEP model runs have been performed with 2017 meteorological conditions. In these model runs, emissions estimated

115 for the years 2005, 2017, and projected for 2030, have been used. The EMEP emissions are used as far as possible, and supplemented by Eclipse (see below) emissions where needed. The model run with 2017 emissions is previously reported in the the 2019 EMEP report (EMEP Status Report 1/2019, 2019). For the EU28 countries (EU28 includes the current EU27 countries and United Kingdom), the official EMEP emissions have been used for both the 2005 and 2017 model runs. For the model run with 2017 emissions, the EMEP emissions are also used for other countries and regions. The 2005 and 2017 EMEP emissions

120 are listed in in appendix B in EMEP Status Report 1/2020 (2020). For the 2030 model runs the emissions for the individual EU28 countries are scaled from the 2005 emissions according to the NEC2030 obligations. The total emissions of NH_3, SO_x

and NO_x in the EU28 countries in 2005, 2017 and 2030 are illustrated in Figure 1a. For all other countries and regions the 2005 and 2030 emissions have been provided by the International Institute for Applied Systems Analysis (IIASA) within the European FP7 project ECLIPSE (http://www.iiasa.ac.at/web/home/research/researchPrograms/air/ECLIPSEv5.html). In this study we use ECLIPSE version 6a (hereafter referred to as 'ECLIPSEv6a'), which is a global emission data-set widely used by the scientific community. Some of the methods used in ECLIPSEv6a are described in the recent publication of Höglund-Isaksson et al. (2020). NH_3 and NO_x emissions from all EU28 countries and selected European non-EU countries are listed in Table 1. For year 2005 EMEP non EU28 and Eclipsev6a emissions are very similar for NO_x, but for NH_3 the EMEP emissions are in general higher.

In order to explore the effects that further emission reductions of NH_3 in 2030 may have on $PM_{2.5}$ concentrations and nitrogen depositions, additional model sensitivity runs have been made. 2030 NH_3 emissions have been reduced by up to 50% in steps of 10%. In addition the 2030 emissions of SO_x and NO_x have been reduced by 10%, and the 2005 NH_3 emissions by 10%. All model runs are listed in Table 2.

4 Model results for 2005 versus 2030

4.1 $PM_{2.5}$

Figure 2 upper panels, shows concentrations of $PM_{2.5}$ as calculated with 2005 emissions (upper left) and 2030 emissions (upper right). The high $PM_{2.5}$ levels over North Africa in both 2005 and in 2030 are caused by large natural sources of mineral dust. As shown in Figure 2, substantial reductions in $PM_{2.5}$ concentrations are expected from 2005 to 2030, caused by reductions in NH_3 emissions, and even larger reductions in SO_x and NO_x emissions, in Europe. Even so, in 2030 elevated $PM_{2.5}$ concentrations still persist in some areas, notably in the Po Valley in Italy and the BeNeLux countries (Belgium, The Netherlands and Luxembourg). In these areas, anthropogenic primary $PM_{2.5}$ and $PM_{2.5}$ precursor emissions are expected to remain high also in 2030. As a result the limit values for $PM_{2.5}$ recommended by WHO (WHO, 2005) are expected to be exceeded in these locations also in 2030.

Figure 1b shows the concentrations of SIA25 averaged over the EU28 countries in 2005, 2017, and 2030 split by component (SO_4^{2-}, NO_3^-, and NH_4^+) Even if the reductions in NH_3 emissions in EU28 are much smaller than the corresponding reductions in SO_x and NO_x, the calculated percentage contributions to SIA25 from NH_4^+ are virtually unchanged between 2005, 2017, and 2030, confirming the findings in Aksoyoglu et al. (2020) for the Payern measurement site in Switzerland. The lack of change in the fraction of NH_4^+ is not surprising, as NH_4^+ is either associated with $(NH_4)_2SO_4$ or with NH_4NO_3. As the molecular weight is 18 g/mol for NH_4, 96 g/mol for SO_4^{2-}, and 62 g/mol for NO_3, the resulting percentage contribution by weight from NH_4 for both NH_4NO_3 and $(NH_4)_2SO_4$ is roughly 25%, consistent with the contributions shown in Figure 1b. Between 2005 and 2017 the percentage reductions in SO_x emissions in EU28 were more that twice as large as the reductions in NO_x, resulting in an increase in the nitrate fraction in SIA25. From 2017 to 2030 the EU28 reductions in NO_x are expected to be larger than for SO_x, resulting in a slight decrease in the fraction of NO_3^-, and a corresponding increase in the SO_4^{2-} fraction in SIA25.

4.2 Deposition of reduced nitrogen

Figure 3 shows the depositions of reduced nitrogen in 2005 (left) and in 2030 (right). As for $PM_{2.5}$, the Po valley and the BeNeLux countries stand out, receiving large amounts of reduced nitrogen depositions both in 2005 and in 2030. The total amount of deposition of reduced nitrogen (and also oxidised nitrogen) per country in 2005, 2017, and 2030 are listed in Table 1. In most central European high emitting countries less reduced nitrogen is deposited than is emitted. Several countries facing the sea, with very few upwind sources, exemplified by Ireland and Portugal, receive far less deposition than they emit. At the same time the Nordic countries (Norway, Sweden, and Finland) and the Baltic countries (Estonia, Latvia, and Lithuania), located downwind of Central Europe, receive more depositions of reduced nitrogen than they emit. For the European Union as a whole, the fraction of deposited over emitted reduced nitrogen is between 0.7 and 0.8 for all 3 emission years considered. The remaining 0.2-0.3 is either deposited at sea or in non-EU countries. About 15% of the NH_3 emitted within the model domain is advected out of the model domain, but much of this is coming from non EU countries close the eastern model boundaries.

As a result of the lower ambitions for reductions in NH_3 emissions compared to NO_x emissions, a larger portion of the total nitrogen deposition is expected to come from NH_3. This is illustrated in Figure 4 which shows the fraction of reduced nitrogen in the total nitrogen deposition calculated with 2005, 2017, and 2030 emissions. The figure shows that this fraction increases significantly from 2005 to 2017, with a further increase expected from 2017 to 2030. By 2030 the percentage of the total nitrogen deposition resulting from NH_3 emissions is expected to exceed 60% in large parts of Europe. The percentage contributions are also listed as an average for EU28, and as averages for individual European countries in Table 1. This underpins the findings from IIASA (2018), that the potential for further reductions of the exceedances of CL for eutrophication is mainly depending on our ability to control future NH_3 emissions. As shown in Figure 5, the calculated CL for eutrophication is exceeded for all three years (2005, 2017, and 2030). Even though the level of exceedance has been substantially reduced from 2005 to 2017, and large reductions in depositions are expected also from 2017 to 2030, the total area in Europe where the CL is exceeded remains high for all three years. The percentage of the area where the CL for eutrophication are exceeded are listed in Table 3 for individual European countries.

4.3 Effects of NH_3 emission controls.

Figures 2c and d show the effects of further 10% reductions of NH_3 emissions on $PM_{2.5}$ concentrations in 2005 and 2030, respectively. Compared to 2005, the absolute effects of 10% further emission reductions in 2030 are smaller. Partially, this is because the percentage emission reductions in 2005 give a larger reduction in absolute numbers compared to percentage emission reductions based on the lower 2030 emissions. As an example, 10% of the emissions from EU in 2005 (3574Gg) will give a smaller reduction than 10% reductions in 2030 (2900Gg). However, these absolute changes in NH_3 emissions are not large enough to explain a decrease of the magnitude seen in Figure 2c versus Figure 2d. As seen in Figure 6, there is more free NH_3, shown as NH_3 over total reduced nitrogen, in 2030 relative to 2005. A larger portion of free NH_3 could partially explain the 2% - 4% annual increase in NH_3 observed by satellites between 2008 and 2018 in countries like Belgium,the Netherlands, France, Germany, Poland, Italy and Spain (Damme et al., 2020). A 10% reduction in NH_3 emissions will make gradually

smaller impact on the formation of NH_4^+ in future years. This is exemplified by the EU28 countries in Table 4. For 2005, we find that as an annual average 10% reductions of NH_3 emissions were about four times more efficient than 10% reductions in NO_X, and almost twice as efficient as SO_x in reducing $PM_{2.5}$ per Gg emitted. For 2030, we find that as an annual average the efficiency mitigating $PM_{2.5}$ concentrations by reducing NH_3 emissions by 10% has been reduced from 0.61 to 0.22 $ngNm^{-3}$ per Gg NH_3 emitted, a reduction of a factor of about 2.6 from 2005. Over the same timespan, the efficiency of a further 10% reduction in NO_x emissions has gone up by about a factor of 1.8 (from 0.15 to 0.27), and by about a factor of 1.6 (0.37 to 0.58) for a 10% further reduction in SO_X emissions.

The dry deposition of NH_3 is faster than that of NH_4^+. As the fraction of NH_3 in total reduced nitrogen increases from 2005 to 2030 (as discussed in Section 4.1), reduced nitrogen may be deposited closer to its sources and potentially increasingly more in the same country as it is emitted. A trend in deposition versus emissions for the individual countries (deposition divided by emissions in Table 1) is not readily seen based on the model calculations. The geographical extent of the countries in Europe is relatively small, and there is considerable variability in the emission trends for NH_3 between the individual EU28 countries, affecting the trends in the depositions also in neighbouring countries.

As a large portion of the emitted reduced nitrogen is deposited close to its sources, changes in emissions close to the EU28 outer geographical borders should affect this fraction more for EU28 as a whole than emission changes in central parts. NH_3 emissions in large EU28 countries as Germany and France have increased between 2005 and 2017, whereas emissions in several countries close to the eastern and southestern geographical EU28 borders, such as Bulgaria, Romania, and Greece, have decreased. For the EU28 countries as a whole the fraction of deposited over emitted reduced nitrogen is between 0.7 and 0.8 for all three years considered (2005, 2017 and 2030). It would be possible to investigate the hypothesis of a possible decrease of the transport distance of reduced nitrogen by looking at so called source receptor matrices for the different years (e.g. studying how the contribution from the country to itself have changed over the years). Such experiments are planned as a follow-up of this paper.

4.3.1 Seasonal effects of NH_3 emission reductions on $PM_{2.5}$

More than 90% of the NH_3 emissions are from agriculture (IIASA, 2020), with low emissions in winter and a maximum in spring, as opposed to both NO_x and SO_x emissions peaking in winter. As a result, there are more SO_4^{2-} and HNO_3 relative to NH_3 in winter than in other seasons. Also the condensation process forming NH_4NO_3 aerosols is favoured by low temperatures. As a result Figure 7 shows that for $PM_{2.5}$ by far the largest effects of further reductions of NH_3 emissions are modelled for the winter months. Notably, most of $PM_{2.5}$ pollution episodes, including exceedances of the EU limits or WHO AQ guidelines for daily mean $PM_{2.5}$ concentrations, are most frequent in large parts of Europe during the winter period (see Tsyro et al. (2019)). The smallest effects are calculated for the summer months, when both SO_x and NO_x emissions are at a minimum. Thus in summer, reductions are mainly confined to the southwestern parts of the North Sea, where ship emissions of NO_x are large. This seasonal behaviour is also seen in the measurements at Preila in Lithuania, with low NH_4^+ concentrations in summer and higher concentrations in the cold season (Davuliene et al., 2021). Furthermore, they found that

the relative abundance of NH_4NO_3 has increased at the expense of $(NH_4)_2SO_4$ as a result of particularly large reductions in SO_x emissions in the last decades.

The seasonal behaviour of $PM_{2.5}$ formation from NH_3 is also demonstrated for EU28 in Table 4 showing that the $PM_{2.5}$ reductions that can be achieved by reducing NH_3 emissions are largest in winter, and are almost constant (and low) for each 10% increment in emission reduction in summer. With a large surplus of free NH_3 in summer the impact of further emission reductions is small. In winter the NH_3 surplus relative to HNO_3 and SO_4^{2-} is much smaller (or nonexistent), and additional NH_3 emission reductions will have larger impacts on $PM_{2.5}$ levels.

4.3.2   Sensitivity tests with additional emission controls.

Figure 8 compares the efficiency of NH_3 emissions reductions on top of the NEC2030 requirements on $PM_{2.5}$ concentrations and reduced nitrogen depositions. Starting from the expected emission levels in 2030, the maps compare the effects of the first 10% reductions (Base - 10%) in NH_3 emissions to the effects of further reductions in NH_3 emissions from 40 - 50% relative to Base. If linear, the effects of these 10% increments in emissions should be equal. However, as shown in Figure 8a, the reductions in $PM_{2.5}$ are larger for the 50%–40% emission reductions compared to Base–10% reductions almost everywhere. This is further demonstrated in Table 4, listing the reductions in annual and seasonal $PM_{2.5}$ concentrations as an average over the EU28 countries in steps of 10% relative to the 2030 NEC emissions. Both as an annual average, and for each season, the reductions in $PM_{2.5}$ increase for each 10% increment. The reductions in $PM_{2.5}$ increase from 0.23 ngm^{-3} per Gg NH_3 emitted for the first 10% additional reductions, to 0.35 ngm^{-3} per Gg emitted for the 50%–40% reductions. The increase in efficiency is a result of a shift in the ratio in NH_3 versus SO_x and NO_x emissions. In Table 4 we also show that with the much higher SO_x and NO_x emissions versus NH_3 emissions, the potential of 10% additional reductions in NH_3 emissions in curbing $PM_{2.5}$ levels was substantially higher in 2005, even when compared to 40%–50% reductions in 2030.

In two additional model runs we separately reduce the 2030 emissions of SO_x and NO_x by 10%. As an annual average we find that 10% reductions in both SO_x and NO_x emissions will lead to larger reductions in $PM_{2.5}$ levels in EU28 than the corresponding 10% reductions in NH_3 emissions. However, as discussed in section 4.3.1, the seasonal variation is large, and in winter reductions of $PM_{2.5}$ per Gg emitted could still be larger for NH_3 than for NO_x.

For depositions of reduced nitrogen the situation is reversed. As shown in Figure 8b the reductions in depositions achieved with NH_3 reduced between 50% and 40% compared to the first 10% reductions are (marginally) smaller in the vicinity of the source regions. This can be explained by a slightly larger portion of the emitted NH_3 being converted to NH_4^+ aerosols having a slower dry deposition rate than NH_3. As a result, the higher deposition seen in the source areas is compensated by a much smaller, but more widespread decrease elsewhere. As discussed in section 4.2, only a small portion of the reduced nitrogen is advected out of the central parts of the model domain.

5 Discussion and Conclusions

Focusing on the effects of NH_3 emissions we have investigated how $PM_{2.5}$ concentrations and depositions of reduced nitrogen will change from 2005 to 2030, assuming that the NEC2030 emission targets will be met. In addition, we have made a sensitivity study for $PM_{2.5}$ for post NEC2030, assuming additional emission reductions on top of the NEC2030 requirements.

Emissions of SO_x and NO_x have decreased in Europe from year 2005 to present, and further emissions reductions are expected by year 2030. However, NH_3 emissions have so far remained high, and projected NEC2030 emission reductions of NH_3 are much smaller than for SO_x and NO_x. Our model calculations show that these differences in emission trends lead to a smaller fraction of the emitted NH_3 being converted to NH_4^+ and an increasingly larger portion of free NH_3 versus NH_4^+ in the atmosphere in Europe. Based on 10% emission reductions of NH_3, NO_x, and SO_x we calculate that the potential for $PM_{2.5}$ formation per Gg NH_3 emitted, is expected to drop by a factor of about 2.6 as an annual average between 2005 and 2030. Over the same timespan the potential for forming $PM_{2.5}$ from NO_x per Gg emitted has increased by a factor of 1.8, and from SO_x by a factor of 1.6 per Gg emitted.

In winter, with low NH_3 emissions and relatively higher NO_x and SO_x emissions, the ratio between NH_3 versus HNO_3 and SO_4^{2-} is higher, and a larger portion of the emitted NH_3 will form particulate NH_4^+. Also, the formation of NH_4NO_3 in equilibrium with HNO_3 and NH_3 is favoured by low temperatures. As a result we find that in winter the effects of further reductions in NH_3 emissions are larger than in other seasons, and comparable to additional reductions in SO_x and NO_x emissions. This is in agreement with the findings in Backes et al. (2016), pointing out that even though the NH_3 emissions are highest in spring and summer due to the application of manure on the fields, emission reductions in winter have a stronger impact on the formation of secondary aerosols than in any other season. Furthermore they stated that the potential of reducing NH_3 emissions in winter is highest through the reduction of animal farming, as this source accounts for about 80% of the NH_3 emissions in the autumn and winter months.

Following the emission reductions of NH_3, deposition of reduced nitrogen is decreasing in Europe. However, the reductions in NO_x emissions are much larger than for NH_3, resulting in a much faster decline in oxidised nitrogen deposition compared to reduced nitrogen. Thus the fraction of reduced over total deposition of nitrogen is increasing, and is expected to reach more than 60% in large parts of Europe by year 2030. Our calculations show that with the existing emission projections the CL for nitrogen will be exceeded in large parts of Europe also in 2030. There are also indications that reduced nitrogen inputs are more effective in decreasing biodiversity than is oxidised nitrogen, as reduced nitrogen is more readily available, stimulating growth of specific plants at the expense others (see van den Berg et al. (2008) and Erisman et al. (2007) and references therein). Furthermore they also suggest that increased levels of NH_4^+ can be toxic to plants (see also Esteban et al. (2016)).

Reducing, and preferably removing, these exceedances, will require larger reduction in nitrogen emissions than currently projected. Given that reduced nitrogen is responsible for the major fraction of nitrogen depositions, the largest cuts should be made in the NH_3 emissions.

As discussed in Nenes et al. (2020, 2021), gas/aerosol partitioning of total reduced and oxidised nitrogen are affected by aerosol pH level and water content, so that low (high) pH is favourable for NH_4^+ (NO_3^-) formation. The increase in the aerosol

fraction in total reduced and oxidised nitrogen would lead to decreases in their dry deposition, and subsequently their residence times and transport distances. This effect has not been accounted for in the EMEP model. Thus some limited local effects might have been missed in our model simulations. For instance, based on the Nenes et al. (2021) results, there may be additional NO_3^- formation in areas with low acidity, such as coastal or dusty regions. Potentially this may reduce the deposition of total nitrate near these local sources, somewhat enhancing the accumulation of particles. Furthermore, as future emissions of SO_x and NO_x are expected to decrease, the pH of the particles is likely to increase, potentially favouring NO_3^- formation, and thus decreasing dry deposition and increasing the transport distances of oxidised and thereby total nitrogen in some regions. On the other hand, our results show that overall, the fraction of reduced nitrogen in the total nitrogen has been increasing, and this increase is expected to continue until 2030. Assuming that the deposition rates for total nitrogen are mostly driven by those of reduced nitrogen (following Nenes et al. (2021)), the local effects of NO_3^- formation bursts would probably not play a major role across the regions in different present and future chemical regimes. Therefore we believe that overall, the main conclusions presented in our paper remain valid.

For many countries the latest source oriented legislation may potentially reduce the emissions of SO_x and NO_x below their emission reduction requirements, and as a result EU28 as a whole could be on track to overshoot the reduction requirements for these species by 2030. But for NH_3 further efforts are needed in order to meet the 2030 commitments for many countries in Europe (IIASA, 2018). Cost-effective measures to further reduce NH_3 emissions differ among various parts of Europe. According to IIASA (2020) the damage cost estimate of 17.50 Euro per kg NH_3 emitted is much higher than the average abatement costs. Also Giannakis et al. (2019) find that much more ambitious commitments for NH_3 emission reductions could be applied by EU-28 countries with relatively minimal costs. According to Giannakis et al. (2019) low emission animal housing would be the least cost effective measure, but still a quarter of the costs of the avoided damage. However, this measure could be the most effective one to reduce emissions in winter, when $PM_{2.5}$ health related limits are the most likely to be exceeded in Europe.

Code availability. The EMEP model version rv4.34 is available as open source code through https://doi.org/10.5281/zenodo.3647990(EMEP MSC-W, 2020).

Data availability. Model results are available upon request to first author

Author contributions. JEJ made the model calculations and wrote most of the paper. HF assisted in designing the model scenarios and in writing the paper. TS calculated the exceedances of critical loads for eutrophication and contributed in the writing of the paper.

11

References

Aksoyoglu, S., Jiang, J., Ciarelli, G., Baltensperger, U., and Prévôt, A. S. H.: Role of ammonia in European air quality with changing land and ship emissions between 1990 and 2030, Atmospheric Chemistry and Physics, 20, 15 665–15 680, https://doi.org/10.5194/acp-20-15665-2020, https://acp.copernicus.org/articles/20/15665/2020/, 2020.

320 Backes, A. M., Aulinger, A., Bieser, J., Matthias, V., and Quante, M.: Ammonia emissions in Europe, part II: How ammonia emission abatement strategies affect secondary aerosols, Atmospheric Environment, 126, 153 – 161, https://doi.org/https://doi.org/10.1016/j.atmosenv.2015.11.039, http://www.sciencedirect.com/science/article/pii/S135223101530546X, 2016.

Binkowski, F. and Shankar, U.: The Regional Particulate Matter Model .1. Model description and preliminary results, J. Geophys. Res., 100,
325 26 191–26 209, 1995.

CLRTAP: Chapter V of Manual on methodologies and criteria for modelling and mapping critical loads and levels and air pollution effects, risks and trends., Tech. rep., UNECE Convention on Long-range Transboundary Air Pollution, https://www.umweltbundesamt.de/en/manual-for-modelling-mapping-critical-loads-levels, 2017.

Colette, A., granier, C., Hodnebrog, Ø., Jacobs, H., Maurizi, A., Nyíri, A., bessagnet, B., D'Angiola, A., D'Isidoro, M., Gauss, M., Meleux,
330 F., Memmesheimer, M., Mieville, A., Rouïl, L., Russo, F., Solberg, S., Stordal, F., and Tampieri, F.: Air quality trends in Europe over the past decade: a first multi-model assessment, Atmos. Chem. Phys., 11, 11 657–11 678, https://doi.org/10.5194/acp-11-11657-2011, http://www.atmos-chem-phys.net/11/11657/2011/, 2011.

Colette, A., Granier, C., Hodnebrog, Ø., Jakobs, H., Maurizi, A., Nyiri, A., Rao, S., Amann, M., Bessagnet, B., D'Angiola, A., Gauss, M., Heyes, C., Klimont, Z., Meleux, F., Memmesheimer, M., Mieville, A., Rouïl, L., Russo, F., Schucht, S., Simpson, D., Stordal, F.,
335 Tampieri, F., and Vrac, M.: Future air quality in Europe: a multi-model assessment of projected exposure to ozone, Atmos. Chem. Phys., 12, 10 613–10 630, https://doi.org/10.5194/acp-12-10613-2012, http://www.atmos-chem-phys.net/12/10613/2012/, 2012.

Damme, M. V., Clarisse, L., Franco, B., Sutton, M. A., Erisman, J. W., Kruit, R. W., van Zanten, M., Whitburn, S., Hadji-Lazaro, J., Hurtmans, D., Clerbaux, C., and Coheur, P.-F.: Global, regional and national trends of atmospheric ammonia derived from a decadal (2008-2018) satellite record, Environmental Research Letters, http://iopscience.iop.org/article/10.1088/1748-9326/abd5e0, 2020.

340 Davuliene, L., Jasineviciene, D., Garbariene, I., Andriejauskiene, J., Ulevicius, V., and Bycenkiene, S.: Long-term air pollution trend analysis in the South-eastern Baltic region, 1981–2017, Atmospheric Research, 247, 105 191, https://doi.org/https://doi.org/10.1016/j.atmosres.2020.105191, http://www.sciencedirect.com/science/article/pii/S0169809520311273, 2021.

De Vries, W., Hettelingh, J.-P., and Posch, M., eds.: Critical Loads and Dynamic Risk Assessments: Nitrogen, Acidity and Metals in Terres-
345 trial and Aquatic Ecosystems, Springer, Dordrecht,, https://doi.org/10.1007/978-94-017-9508-1, 2015.

EEA: Effects of air pollution on European ecosystems, Tech. Rep. EEA 11/2014, available from www.eea.europa.eu/publications, European Environment Agency, Copenhagen, Denmark, https://doi.org/10.2800/18365, 2014.

EMEP Status Report 1/2019: Transboundary particulate matter, photo-oxidants, acidifying and eutrophying components, EMEP MSC-W & CCC & CEIP, https://emep.int/publ/reports/2019/EMEP_Status_Report_1_2019.pdf, Norwegian Meteorological Institute (EMEP/MSC-
350 W), Oslo, Norway, 2019.

EMEP Status Report 1/2020: Transboundary particulate matter, photo-oxidants, acidifying and eutrophying components, EMEP MSC-W & CCC & CEIP, https://emep.int/publ/reports/2020/EMEP_Status_Report_1_2020.pdf, Norwegian Meteorological Institute (EMEP/MSC-W), Oslo, Norway, 2020.

Erisman, J., Bleeker, A., Galloway, J., and Sutton, M.: Reduced nitrogen in ecology and the environment, Environmental Pollution, 150, 140–149, https://doi.org/https://doi.org/10.1016/j.envpol.2007.06.033, https://www.sciencedirect.com/science/article/pii/S0269749107003089, 2007.

Esteban, R., Ariz, I., Cruz, C., and Moran, J. F.: Review: Mechanisms of ammonium toxicity and the quest for tolerance, Plant Science, 248, 92–101, https://doi.org/https://doi.org/10.1016/j.plantsci.2016.04.008, https://www.sciencedirect.com/science/article/pii/S0168945216300619, 2016.

Gauss, M., Tsyro, S., Fagerli, H., Hjellbrekke, A.-G., Aas, W., and Solberg, S.: EMEP MSC-W model performance for acidifying and eutrophying components, photo-oxidants and particulate matter in 2015., Supplementary material to EMEP Status Report 1/2017, available online at www.emep.int, The Norwegian Meteorological Institute, Oslo, Norway, 2017.

Gauss, M., Tsyro, S., Fagerli, H., Hjellbrekke, A.-G., Aas, W., and Solberg, S.: EMEP MSC-W model performance for acidifying and eutrophying components, photo-oxidants and particulate matter in 2016., Supplementary material to EMEP Status Report 1/2018, available online at www.emep.int, The Norwegian Meteorological Institute, Oslo, Norway, 2018.

Gauss, M., Tsyro, S., Benedictow, A., Fagerli, H., Hjellbrekke, A.-G., Aas, W., and Solberg, S.: EMEP MSC-W model performance for acidifying and eutrophying components, photo-oxidants and particulate matter in 2017., Supplementary material to EMEP Status Report 1/2019, available online at www.emep.int, The Norwegian Meteorological Institute, Oslo, Norway, 2019.

Gauss, M., Tsyro, S., Benedictow, A., Hjellbrekke, A.-G., Aas, W., and Solberg, S.: EMEP MSC-W model performance for acidifying and eutrophying components, photo-oxidants and particulate matter in 2018., Supplementary material to EMEP Status Report 1/2020, available online at www.emep.int, The Norwegian Meteorological Institute, Oslo, Norway, 2020.

Ge, Y., Heal, M. R., Stevenson, D. S., Wind, P., and Vieno, M.: Evaluation of global EMEP MSC-W (rv4.34) WRF (v3.9.1.1) model surface concentrations and wet deposition of reactive N and S with measurements, Geoscientific Model Development, 14, 7021–7046, https://doi.org/10.5194/gmd-14-7021-2021, https://gmd.copernicus.org/articles/14/7021/2021/, 2021.

Giannakis, E., Kushta, J., Bruggeman, A., and Llieveld, J.: Costs andf benefits of agriculural ammonia emission abatement options for complience with European air quality regulations, Environmental Sciences Europe, https://doi.org/10.1186/s12302-019-0275-0, https://enveurope.springeropen.com/articles/10.1186/s12302-019-0275-0, 2019.

Hettelingh, J.-P., Posch, M., and de Smet, P. e.: Multi-effect critical loads used in multi-pollutant reduction agreements in Europe, Water, Air and Soil Pollution, 130, 1133–1138, 2001.

Hettelingh, J.-P., Posch, M., and Slootweg, J.: European critical loads: database, biodiversity and ecosystems at risk., https://doi.org/10.21945/RIVM-2017-0155, CCE Final Report 2017. RIVM Report 2017-0155, 2017.

Höglund-Isaksson, L., Gómez-Sanabria, A., Klimont, Z., Rafaj, P., and Schöpp, W.: Technical potentials and costs for reducing global anthropogenic methane emissions in the 2050 timeframe –results from the GAINS model, Environmental Research Communications, 2, 025 004, https://doi.org/10.1088/2515-7620/ab7457, https://doi.org/10.1088%2F2515-7620%2Fab7457, 2020.

IIASA: Progress towards the achievement of the EU's air quality and emissions objectives, Tech. rep., IIASA (International Institute for Applied Systems Analysis), https://ec.europa.eu/environment/air/pdf/clean_air_outlook_overview_report.pdf, 2018.

IIASA: Assessment Report on Ammonia 2020. Draft April 2020, Tech. rep., IIASA (International Institute for Applied Systems Analysis), https://iiasa.ac.at/web/home/research/researchPrograms/air/policy/Assessment_Report_on_Ammonia_20200410.pdf, 2020.

Jiang, J., Aksoyoglu, S., Ciarelli, G., Baltensperger, U., and Prévôt, A. S.: Changes in ozone and PM2.5 in Europe during the period of 1990–2030: Role of reductions in land and ship emissions, Science of The Total Environment, 741, 140 467, https://doi.org/https://doi.org/10.1016/j.scitotenv.2020.140467, https://www.sciencedirect.com/science/article/pii/S0048969720339899, 2020.

Jonson, J. E., Schulz, M., Emmons, L., Flemming, J., Henze, D., Sudo, K., Tronstad Lund, M., Lin, M., Benedictow, A., Koffi, B., Dentener, F., Keating, T., Kivi, R., and Davila, Y.: The effects of intercontinental emission sources on European air pollution levels, Atmospheric Chemistry and Physics, 18, 13 655–13 672, https://doi.org/10.5194/acp-18-13655-2018, https://www.atmos-chem-phys.net/18/13655/2018/, 2018.

Karl, M., Jonson, J. E., Uppstu, A., Aulinger, A., Prank, M., Jalkanen, J.-P., Johansson, L., Quante, M., and Matthias, V.: Effects of ship emissions on air quality in the Baltic Sea region simulated with three different chemistry transport models, Atmospheric Chemistry and Physics Discussions, 2019, 1–48, https://doi.org/10.5194/acp-2018-1317, https://www.atmos-chem-phys-discuss.net/acp-2018-1317/, 2019.

Metzger, S., Steil, B., Abdelkader, M., Klingmüller, K., Xu, L., Penner, J. E., Fountoukis, C., Nenes, A., and Lelieveld, J.: Aerosol water parameterisation: a single parameter framework, Atmospheric Chemistry and Physics, 16, 7213–7237, https://doi.org/10.5194/acp-16-7213-2016, https://www.atmos-chem-phys.net/16/7213/2016/, 2016.

Metzger, S., Abdelkader, M., Steil, B., and Klingmüller, K.: Aerosol water parameterization: long-term evaluation and importance for climate studies, Atmospheric Chemistry and Physics, 18, 16 747–16 774, https://doi.org/10.5194/acp-18-16747-2018, https://www.atmos-chem-phys.net/18/16747/2018/, 2018.

Nenes, A., Pandis, S. N., Weber, R. J., and Russell, A.: Aerosol pH and liquid water content determine when particulate matter is sensitive to ammonia and nitrate availability, Atmospheric Chemistry and Physics, 20, 3249–3258, https://doi.org/10.5194/acp-20-3249-2020, https://acp.copernicus.org/articles/20/3249/2020/, 2020.

Nenes, A., Pandis, S. N., Kanakidou, M., Russell, A. G., Song, S., Vasilakos, P., and Weber, R. J.: Aerosol acidity and liquid water content regulate the dry deposition of inorganic reactive nitrogen, Atmospheric Chemistry and Physics, 21, 6023–6033, https://doi.org/10.5194/acp-21-6023-2021, https://acp.copernicus.org/articles/21/6023/2021/, 2021.

Nilsson, J. and Grennfelt, P., eds.: Critical Loads for Sulphur and Nitrogen, Nordic Council of Ministers, Copenhagen, Denmark, Nord 1988;97, 418pp., 1988.

Petit, J.-E., Amodeo, T., Meleux, F., Bessagnet, B., Menut, L., Grenier, D., Pellan, Y., Ockler, A., Rocq, B., Gros, V., Sciare, J., and Favez, O.: Characterising an intense PM pollution episode in March 2015 in France from multi-site approach and near real time data: Climatology, variabilities, geographical origins and model evaluation, Atmospheric Environment, 155, 68 – 84, https://doi.org/https://doi.org/10.1016/j.atmosenv.2017.02.012, http://www.sciencedirect.com/science/article/pii/S1352231017300821, 2017.

Posch, M., Hettelingh, J.-P., and De Smet, P.: Characterization of critical load exceedances in Europe, Water, Air and Soil Pollution, 130, 1139–1144, 2001.

Reis, S., Grennfelt, P., Klimont, Z., Amann, M., ApSimon, H., Hettelingh, J., Holland, M., Le Gall, A., Maas, R., Posch, M., Spranger, T., Sutton, M., and Williams, M.: From acid rain to climate change, Science, 338, 1.153–1.154, https://doi.org/10.1126/science.1226514, 2012.

Seinfeld, J. and Pandis, S.: Atmospheric chemistry and physics. From air polluition to climate change, John Wiley & Sons, Inc, 2016.

Simpson, D., Benedictow, A., Berge, H., Bergström, R., Emberson, L., Fagerli, H., Flechard, C., Hayman, G., Gauss, M., Jonson, J., Jenkin, M., Nyíri, A., Richter, C., Semeena, V., Tsyro, S., Tuovinen, J.-P., Valdebenito, A., and Wind, P.: The EMEP MSC-W chemical transport model – technical description, Atmos. Chem. Phys., 12, 7825–7865, https://doi.org/10.5194/acp-12-7825-2012, 2012.

Simpson, D., Bergström, Tsyro, S., and Wind, P.: Updates to the EMEP MSC-W model, 2019 – 2020, in: Transboundary particulate matter, photo-oxidants, acidifying and eutrophying components. EMEP Status Report 1/2020, pp. 155–165, The Norwegian Meteorological Institute, Oslo, Norway, 2020.

Slootweg, J., Posch, M., and Hettelingh (eds.), J.: Modelling and mapping the impacts of atmospheric deposition of nitrogen and sulphur, Tech. rep., CCE Status Report 2015. RIVM Report 2015-0193, Coordination Centre for Effects, Bilthoven, Netherlands, 182 pp, available at www.wge-cce.org, 2015.

Theobald, M. R., Vivanco, M. G., Aas, W., Andersson, C., Ciarelli, G., Couvidat, F., Cuvelier, K., Manders, A., Mircea, M., Pay, M.-T., Tsyro, S., Adani, M., Bergström, R., Bessagnet, B., Briganti, G., Cappelletti, A., D'Isidoro, M., Fagerli, H., Mar, K., Otero, N., Raffort, V., Roustan, Y., Schaap, M., Wind, P., and Colette, A.: An evaluation of European nitrogen and sulfur wet deposition and their trends estimated by six chemistry transport models for the period 1990–2010, Atmospheric Chemistry and Physics, 19, 379–405, https://doi.org/10.5194/acp-19-379-2019, https://acp.copernicus.org/articles/19/379/2019/, 2019.

Tsyro, S. and Metzgert, S.: EQSAM4clim, in: Transboundary particulate matter, photo-oxidants, acidifying and eutrophying components. EMEP Status Report 1/2019, pp. 133–141, The Norwegian Meteorological Institute, Oslo, Norway, 2019.

Tsyro, S., Aas, W., Solberg, S., Benedictow, A., Fagerli, H., and Scheuschner, T.: Status of transboundary air pollution in 2017, in: Transboundary particulate matter, photo-oxidants, acidifying and eutrophying components. EMEP Status Report 1/2019, pp. 17–42, The Norwegian Meteorological Institute, Oslo, Norway, 2019.

Tsyro, S., Aas, W., Solberg, S., Benedictow, A., Fagerli, H., and Scheuschner, T.: Status of transboundary air pollution in 2018, in: Transboundary particulate matter, photo-oxidants, acidifying and eutrophying components. EMEP Status Report 1/2020, pp. 17–34, The Norwegian Meteorological Institute, Oslo, Norway, 2020.

van den Berg, L., Peters, C., Ashmore, M., and Roelofs, J.: Reduced nitrogen has a greater effect than oxidised nitrogen on dry heathland vegetation, Environmental Pollution, 154, 359–369, https://doi.org/https://doi.org/10.1016/j.envpol.2007.11.027, https://www.sciencedirect.com/science/article/pii/S0269749107005891, reduced Nitrogen in Ecology and the Environment, 2008.

Vieno, M., Heal, M. R., Twigg, M. M., MacKenzie, I. A., Braban, C. F., Lingard, J. J. N., Ritchie, S., Beck, R. C., Móring, A., Ots, R., Marco, C. F. D., Nemitz, E., Sutton, M. A., and Reis, S.: The UK particulate matter air pollution episode of March–April 2014: more than Saharan dust, Environmental Research Letters, 11, 044 004, https://doi.org/10.1088/1748-9326/11/4/044004, https://doi.org/10.1088%2F1748-9326%2F11%2F4%2F044004, 2016.

Vivanco, M. G., Theobald, M. R., García-Gómez, H., Garrido, J. L., Prank, M., Aas, W., Adani, M., Alyuz, U., Andersson, C., Bellasio, R., Bessagnet, B., Bianconi, R., Bieser, J., Brandt, J., Briganti, G., Cappelletti, A., Curci, G., Christensen, J. H., Colette, A., Couvidat, F., Cuvelier, C., D'Isidoro, M., Flemming, J., Fraser, A., Geels, C., Hansen, K. M., Hogrefe, C., Im, U., Jorba, O., Kitwiroon, N., Manders, A., Mircea, M., Otero, N., Pay, M.-T., Pozzoli, L., Solazzo, E., Tsyro, S., Unal, A., Wind, P., and Galmarini, S.: Modeled deposition of nitrogen and sulfur in Europe estimated by 14 air quality model systems: evaluation, effects of changes in emissions and implications for habitat protection, Atmospheric Chemistry and Physics, 18, 10 199–10 218, https://doi.org/10.5194/acp-18-10199-2018, https://www.atmos-chem-phys.net/18/10199/2018/, 2018.

WHO: Air quality guidelines. Global update 2005. Particulate matter, ozone, nitrogen dioxide and sulfur dioxide, http://www.who.int/phe/ health_topics/outdoorair/outdoorair_aqg/en/, World Health Organisation, European Centre for Environment and Health Bonn Office, ISBN 92 890 2192, 2005.

Table 1. Emissions of NO_x and NH_3, depositions of oxidised and reduced nitrogen, and the ratio of reduced versus total (reduced + oxidised) deposition of nitrogen (Red fr). Emissions and deposition are listed in 100 Mg of N. (Bosnia H. is Bosnia and Herzegovina and N. Macedonia is North Macedonia. UK is The United Kingdom of Great Britain and Northern Ireland.)

| Country | 2005 | | | | | 2017 | | | | | 2030 | | | | |
| | Emissions | | Depositions | | Red fr | Emissions | | Depositions | | Red fr | Emissions | | Depositions | | Red fr |
	NO_x	NH_3	ox.N	red.N		NO_x	NH_3	ox.N	red.N		NO_x	NH_3	ox.N	red.N	
						28 EU countries									
Austria	724	516	631	589	48	441	569	423	587	58	224	454	261	487	65
Belgium	968	620	326	339	51	536	550	218	320	59	397	539	144	299	67
Bulgaria	581	425	552	444	45	313	407	400	451	53	245	374	310	408	57
Croatia	265	392	412	370	47	167	310	281	331	54	114	294	198	306	57
Cyprus	64	62	26	20	43	46	53	23	22	49	29	49	21	22	51
Czechia	840	636	669	587	47	496	552	462	555	55	303	496	283	465	62
Denmark	627	729	295	359	55	340	629	212	319	60	200	554	134	277	67
Estonia	128	84	168	108	39	100	84	133	104	44	89	84	98	95	49
Finland	633	307	628	351	36	396	256	505	347	41	335	246	361	281	44
France	4322	4980	2939	3423	54	2456	4994	1899	3393	64	1340	4333	1199	3054	72
Germany	4821	5267	3542	3943	53	3616	5544	2493	4010	62	1687	3740	1501	3039	67
UK	5408	2343	1315	1177	47	2718	2332	844	1148	58	1460	1968	518	1042	67
Greece	1430	533	657	337	34	776	459	443	336	43	644	479	402	336	46
Hungary	536	709	595	560	48	362	722	421	550	57	114	482	274	442	62
Ireland	517	933	146	392	73	335	976	107	414	79	769	887	67	379	85
Italy	3896	3515	2258	2215	50	2158	3164	1467	2008	58	1364	2953	1081	1923	64
Latvia	128	123	267	202	43	113	136	219	209	49	85	122	152	179	54
Lithuania	189	257	311	300	49	161	243	254	297	54	93	231	172	266	61
Luxembourg	167	48	26	26	50	55	48	15	26	63	28	38	9	22	71
Malta	30	12	2	1	33	15	9	2	2	50	6	9	2	1	33
Netherlands	1242	1274	410	554	57	767	1088	308	545	64	484	1006	191	459	71
Poland	2645	2671	2406	2303	49	2447	2533	1945	2240	54	1614	2217	1237	1908	61
Portugal	816	516	306	242	44	484	474	216	233	52	302	439	146	219	60
Romania	992	1697	1192	1265	51	706	1353	888	1164	57	397	1273	640	1062	62
Slovakia	313	312	352	303	46	201	219	249	268	51	157	219	167	236	62
Slovenia	167	166	173	136	44	107	153	117	146	56	16	119	69	112	62
Spain	4151	4173	1866	1699	48	2249	4267	1167	2044	64	416	3388	667	1570	70
Sweden	560	477	931	610	40	377	439	746	680	48	190	396	478	491	51
EU28	32848	29440	23401	22855	49	22938	32562	16457	22648	58	12131	23882	10782	19380	64
						non EU countries									
Switzerland	280	497	257	343	57	186	454	171	373	69	189	446	123	302	71
Iceland	88	26	39	26	40	70	43	43	37	46	17	33	28	25	47
Norway	660	179	486	247	34	496	275	408	307	43	281	192	274	214	44
Albania	76	138	123	86	41	76	199	92	124	57	72	197	78	103	57
Turkey	2042	2355	2382	1626	41	2389	6092	2139	3822	64	2421	3992	2074	2555	55
Bosnia H.	100	130	286	225	44	94	175	198	240	55	103	205	147	215	59
N. Macedonia	113	65	121	69	36	73	84	80	76	49	73	58	70	65	48
Serbia	508	467	502	389	44	450	535	359	432	55	213	250	198	306	61
Montenegro	24	19	55	39	41	43	17	42	35	45	13	16	33	37	53

Table 2. Model runs performed. All model runs have been performed with 2017 meteorological conditions as described in Section 3. Base denotes model runs with all emissions for the years 2005, 2017, and 2030. For 2005 emissions in EU28 are based on EMEP 2005 official emissions. Remaining land-based emissions from ECLIPSEv6a. For 2017 all emissions are as reported in EMEP Status Report 1/2020 (2020) appendix B. For 2030 EU28 emissions are scaled according to the NEC2030 obligations based on the 2005 emissions. Remaining land based emissions from Eclipse v6a. Emissions and model runs are also described in section 3. The additional model sensitivity runs reducing the emissions in steps of 10% are also listed.

| Year | Base | percentage emission reductions | | | | | | |
| | | NH_3 | | | | | NO_x | SO_x |
		-10%	-20%	-30%	-40%	-50%	-10%	-10%
2005	√	√	√				√	√
2017	√							
2030	√	√	√	√	√	√	√	√

Table 3. Exceedance of CL for Eutrophication (CLex eut.) by deposition (Dep.) of total nitrogen. Exceedance are expressed as share [%] of the receptor area.

Country	Eco Area 1000 km2	CLex eut.[%] 2005	2017	2030
28 EU countries				
Austria	50.4	73.5	56.6	29.7
Belgium	9.2	100.0	100.0	99.5
Bulgaria	48.9	99.9	99.5	98.1
Croatia	32.7	99.0	94.3	84.6
Cyprus	1.6	100.0	100.0	100.0
Czechia	6.4	100.0	99.6	86.1
Denmark	5.1	100.0	100.0	97.9
Estonia	18.9	80.6	75.7	42.0
Finland	40.9	10.2	7.8	0.9
France	176.3	78.0	62.0	46.1
Germany	101.3	83.6	77.0	64.7
Greece	64.4	98.0	94.1	93.2
Hungary	22.8	98.3	96.5	77.3
Ireland	12.8	25.0	22.2	14.8
Italy	105.7	77.6	60.0	48.7
Latvia	30.7	96.9	95.1	78.2
Lithuania	19.1	99.7	99.2	96.3
Luxembourg	1.0	100.0	100.0	100.0
Malta	<1	94.8	94.8	94.8
Netherlands	0.4	85.2	78.3	70.0
Poland	91.2	78.2	70.8	48.5
Portugal	33.9	98.5	93.0	85.4
Romania	95.0	96.5	93.8	82.7
Slovakia	21.8	99.8	98.3	92.5
Slovenia	10.5	100.0	99.8	87.8
Spain	195.8	99.7	98.2	95.2
Sweden	58.6	14.3	12.8	8.4
United Kingdom	54.3	32.5	18.0	9.2
EU28	1,309.7	80.4	73.3	62.5
non EU countries				
Albania	17.4	88.3	87.0	81.8
Belarus	55.0	100.0	100.0	99.3
Bosnia & Herzegovina	29.7	87.3	80.0	81.8
Kosovo	4.0	75.7	66.6	55.3
Liechtenstein	<1	100.0	99.6	100.0
North Macedonia	13.1	79.9	69.9	61.9
Moldova, Rep. of	3.4	88.0	87.7	73.3
Montenegro	7.0	77.8	67.1	60.7
Norway	302.6	11.8	10.1	3.8
Russia	607.2	56.8	54.0	39.6
Serbia	28.9	94.8	89.8	75.4
Switzerland	7.5	82.1	74.3	55.5
Ukraine	91.2	99.8	99.8	98.6
Europe	2,476.8	67.7	62.8	52.3

Table 4. First column listing annual and seasonal concentrations of $PM_{2.5}$ as an average for the EU28 countries. Column 2 - 5 are listing the EU28 average reductions calculated in steps of 10% reductions in NH_3 emissions. For $PM_{2.5}$ the reductions in $ngNm^{-3}$ per Gg of reduction of NH_3 emissions are shown In brackets. The Corresponding effects of 10 and 20% reductions of NH_3 emissions in 2005 are also shown. The effects of 10% reductions of SO_x and NO_x emissions in 2030 are also listed. The reductions in $PM_{2.5}$ in $ngNm^{-3}$ per Gg emitted are given in brackets with NH_3 counted as NH_3 with molecular weight 17), NO_x counted as NO_2 with molecular weight 46 and SO_x counted as SO_2 with molecular weight 64.

Season	Conc. μgm^{-3}	10% – Base μgm^{-3}	20% – 10% μgm^{-3}	30% – 20% μgm^{-3}	40% - 30% μgm^{-3}	50% – 40% μgm^{-3}
$PM_{2.5}$ 2030, NH_3 reductions						
Annual	4.45	-0.066 (0.23)	-0.074 (0.26)	-0.082 (0.28)	-0.092 (0.32)	-0.103 (0.35)
Winter	5.31	-0.126 (0.44)	-0.142 (0.49)	-0.160 (0.55)	-0.180 (0.62)	-0.202 (0.70)
Spring	3.90	-0.055 (0.19)	-0.061 (0.21)	-0.068 (0.23)	-0.77 (0.26)	-0.087 (0.30)
Summer	4.23	-0.015 (0.05)	-0.016 (0.06)	-0.016 (0.06)	-0.017 (0.06)	-0.018 (0.07)
Autumn	4.39	-0.069 (0.24)	-0.076 (0.26)	-0.086 (0.30)	-0.096 (0.33)	-0.108 (0.37)
$PM_{2.5}$ 2030, NO_x reductions						
Annual	4.45	-0.094 (0.27)				
Winter	5.31	-0.112 (0.32)				
Spring	3.90	-0.105 (0.30)				
Summer	4.23	-0.051 (0.15)				
Autumn	4.39	-0.106 (0.38)				
$PM_{2.5}$ 2030, SO_x reductions						
Annual	4.45	-0.085 (0.58)				
Winter	5.31	-0.101 (0.69)				
Spring	3.90	-0.082 (0.56)				
Summer	4.23	-0.071 (0.48)				
Autumn	4.39	-0.086 (0.59)				
$PM_{2.5}$ 2005, NH_3 reductions						
Annual	8.87	-0.22 (0.61)	-0.23 (0.64)			
$PM_{2.5}$ 2005, NOx reductions						
Annual	8.87	-0.16 (0.15)				
$PM_{2.5}$ 2005, SO_x reductions						
Annual	8.87	-0.24 (0.37)				

a) Emis. in Gg y^{-1} in EU28
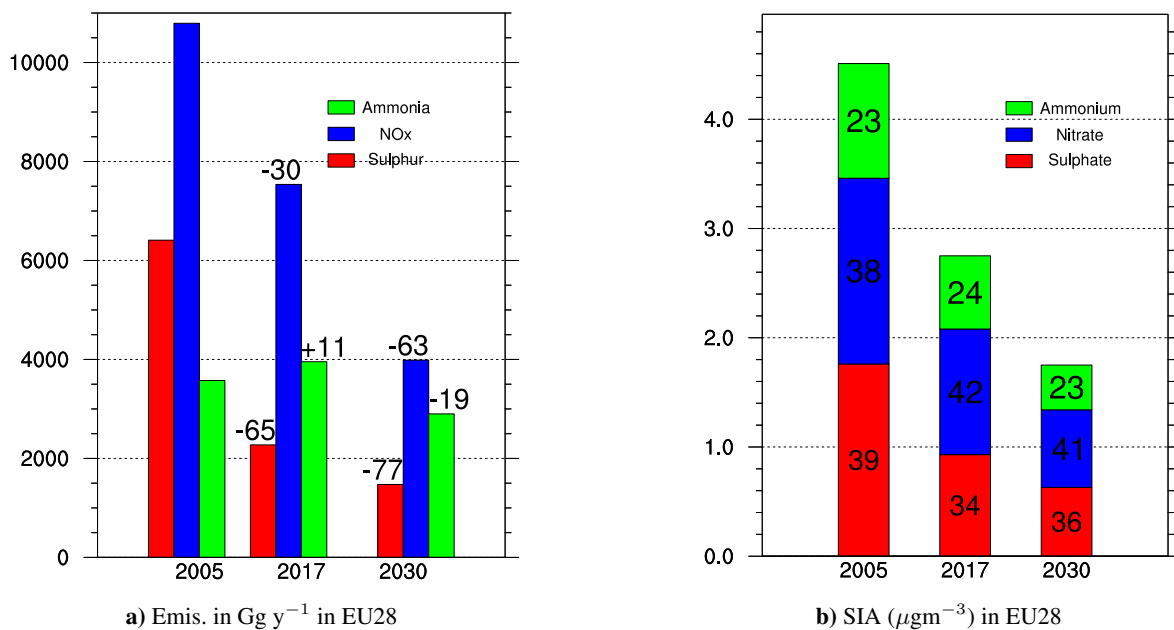
b) SIA (μgm^{-3}) in EU28

Figure 1. a: Emissions of SO$_x$ as SO$_2$, NO$_x$ as NO$_2$, and NH$_3$ summed up for the EU28 countries. Percentage change in emissions from 2005 are given above the bars. b: Concentrations of SIA (μgm^{-3}) split into sulphate (SO$_4^{2-}$), nitrate (NO$_3^-$), and ammonium (NH$_4^+$) and averaged over the EU28 countries. Percentage contributions to SIA are printed inside the bars.
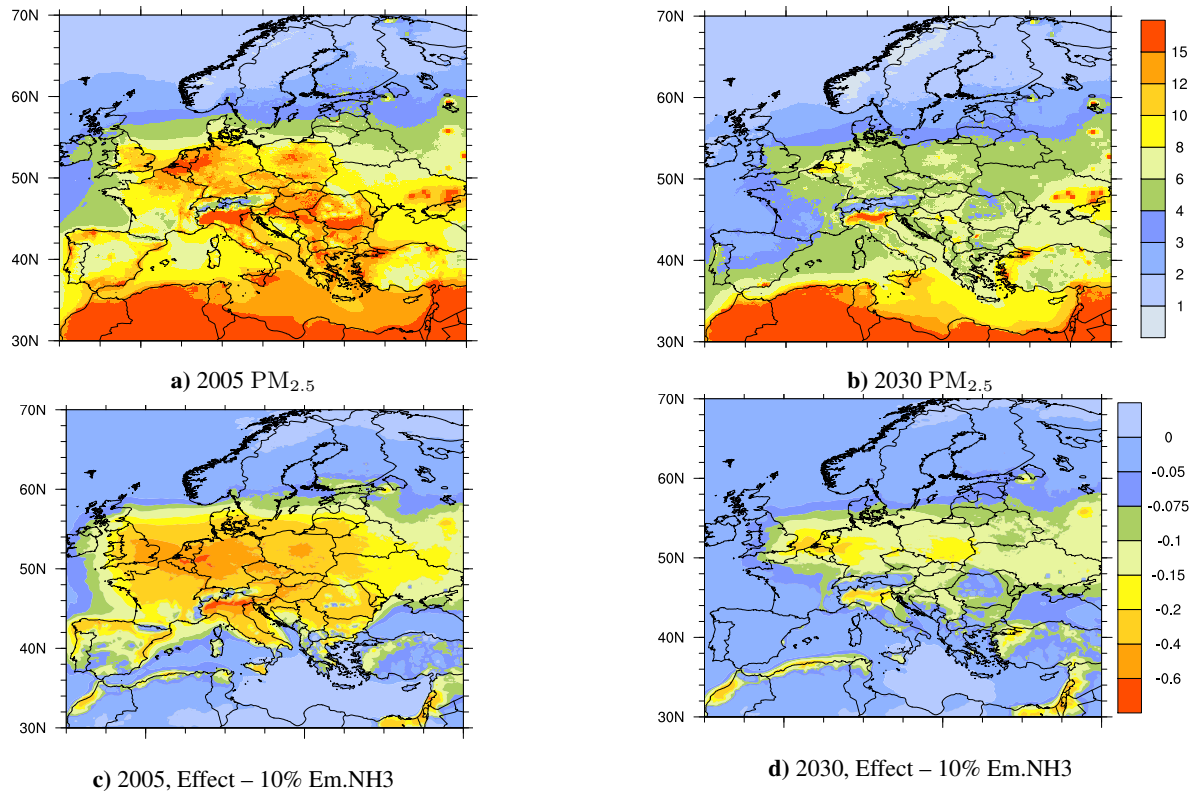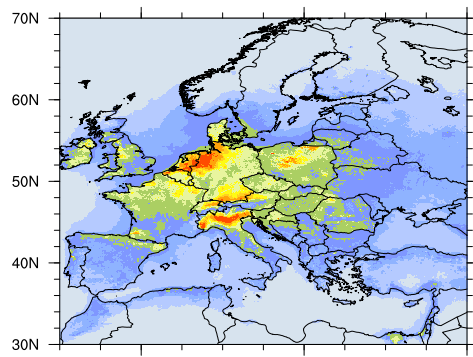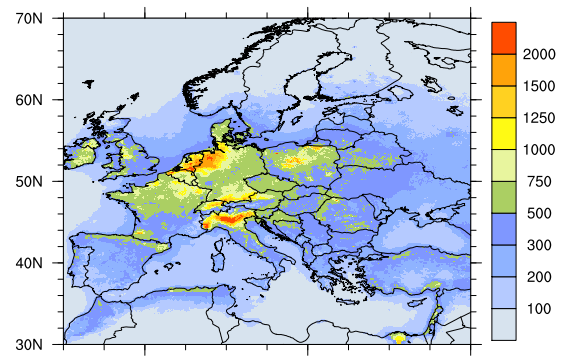
a) 2005 $PM_{2.5}$

b) 2030 $PM_{2.5}$

c) 2005, Effect – 10% Em.NH3

d) 2030, Effect – 10% Em.NH3

Figure 2. $PM_{2.5}$ in 2005 (a), and in 2030 (b). Effects of 10% further reductions in NH_3 emissions in 2005 (c) and in 2030 (d) [μgm^{-3}].

a) 2005 dep. of reduced N

b) 2030 dep. of reduced N

Figure 3. Deposition of reduced N in 2005 (a) and in 2030 (b) $[\mathrm{mg(N)m^{-2}y^{-1}}]$.

a) 2005, Frac redN/totN

b) 2017, Frac redN/totN

c) 2030, Frac redN/totN
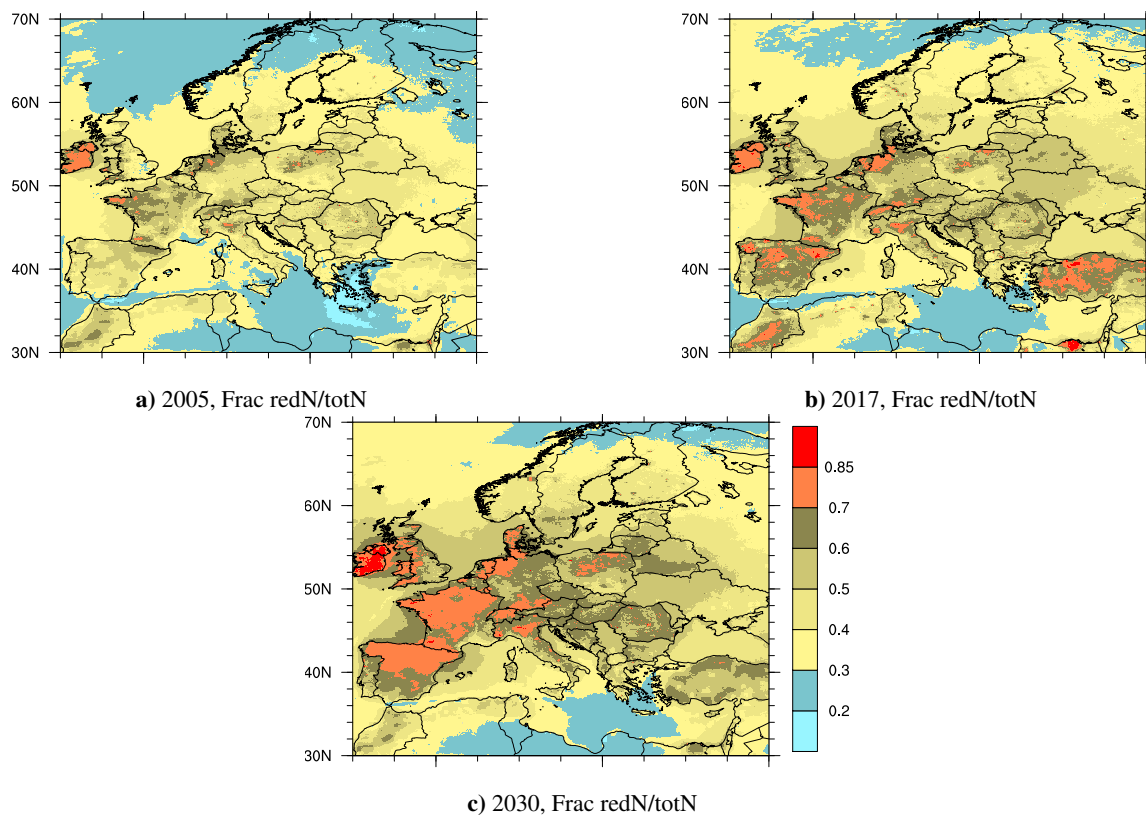
Figure 4. Fraction of reduced N deposition relative to total N (reduced pluss oxidised nitrogen) deposition, calculated with year 2005, 2017 and 2030 emissions.

a) Exceedances in 2005

b) Exceedances in 2017

c) Exceedances in 2030
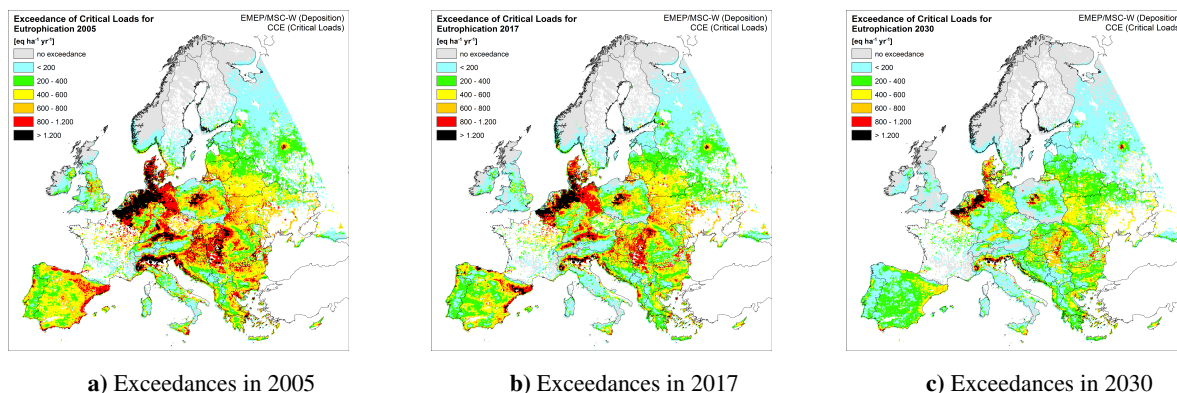
Figure 5. Calculated exceedanses of CL for eutrophication (eq ha^{-1}y^{-1}) in 2005, 2017, and 2030.

a) 2005, Frac NH$_3$ in redN

b) 2017, Frac NH$_3$ in redN

c) 2030, Frac NH$_3$ in redN
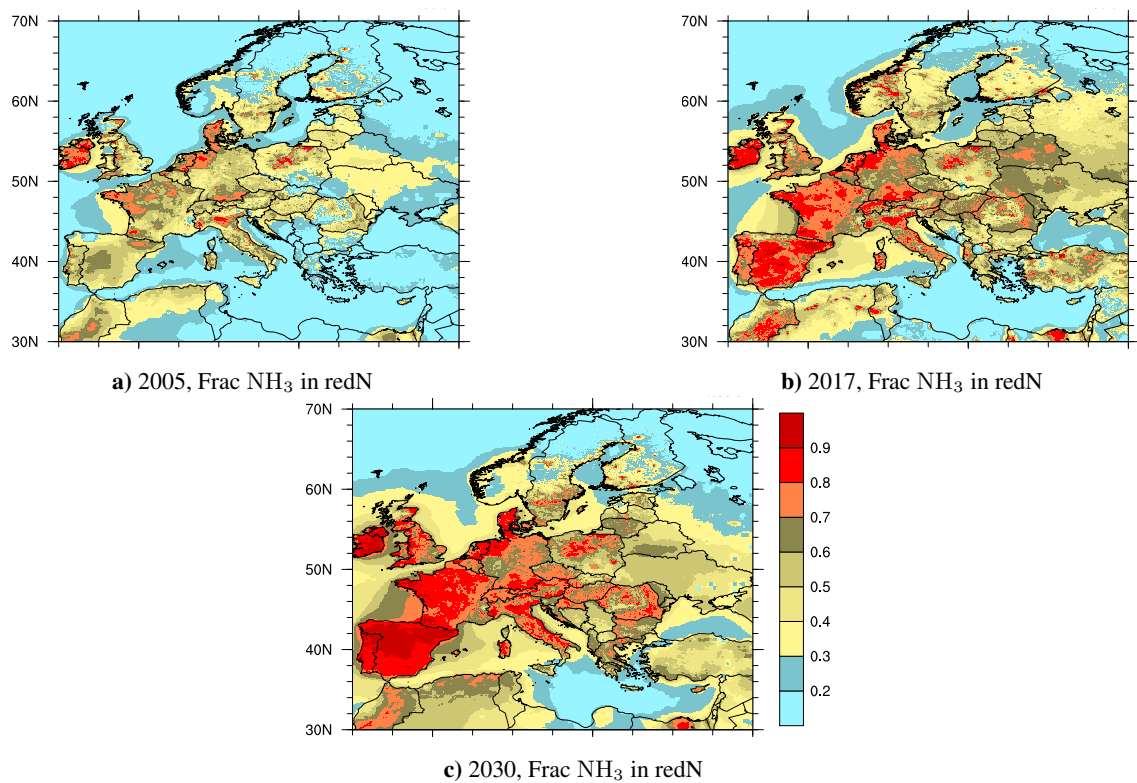
Figure 6. Fraction of NH$_3$ in reduced nitrogen (NH$_3$ + NH$_4^+$) in 2005, 2017, and 2030.
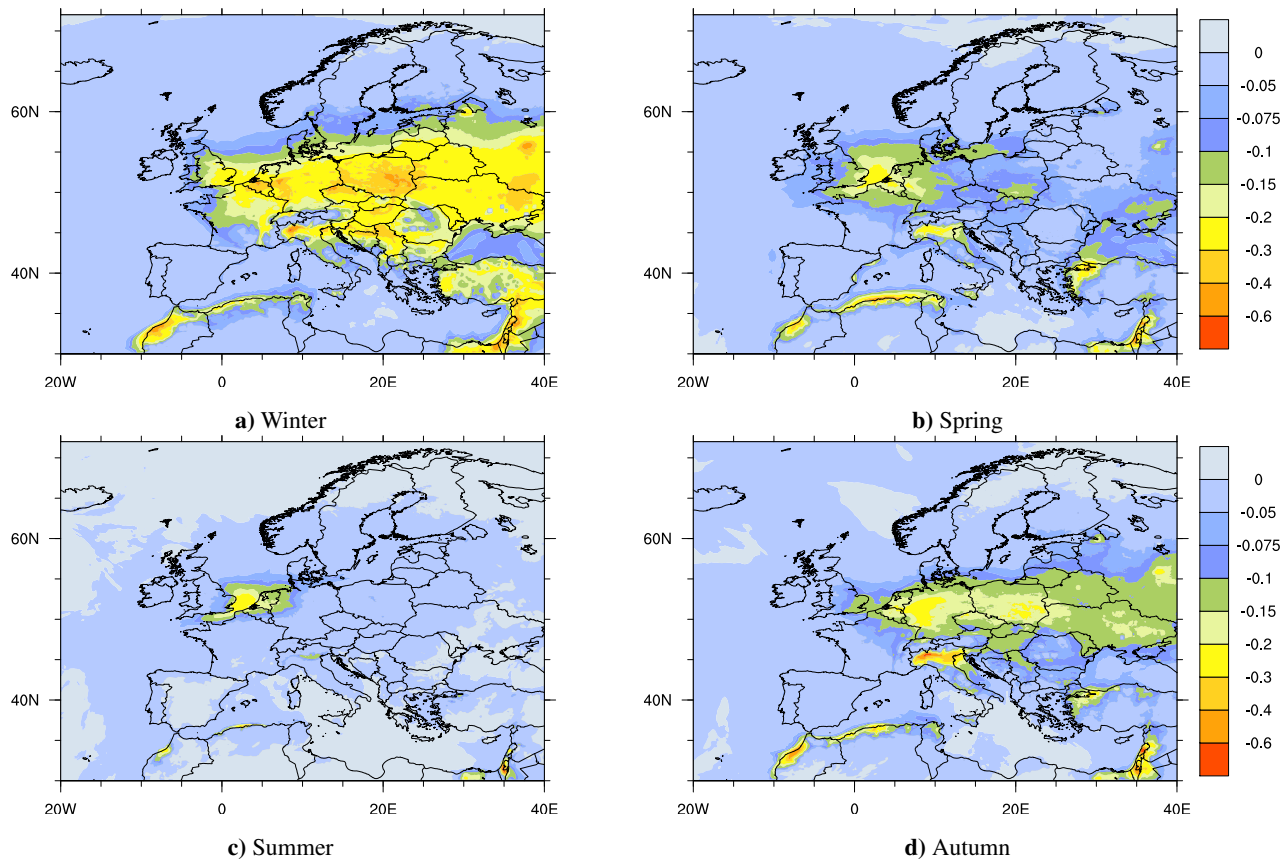
Figure 7. Effects of a 10% decrease in 2030 NH$_3$ emissions on PM$_{2.5}$ [μgm^{-3}] split by season. Winter: December, January, February. Spring: March, April, May. Summer: June, July, August. Autumn: September, October, November.
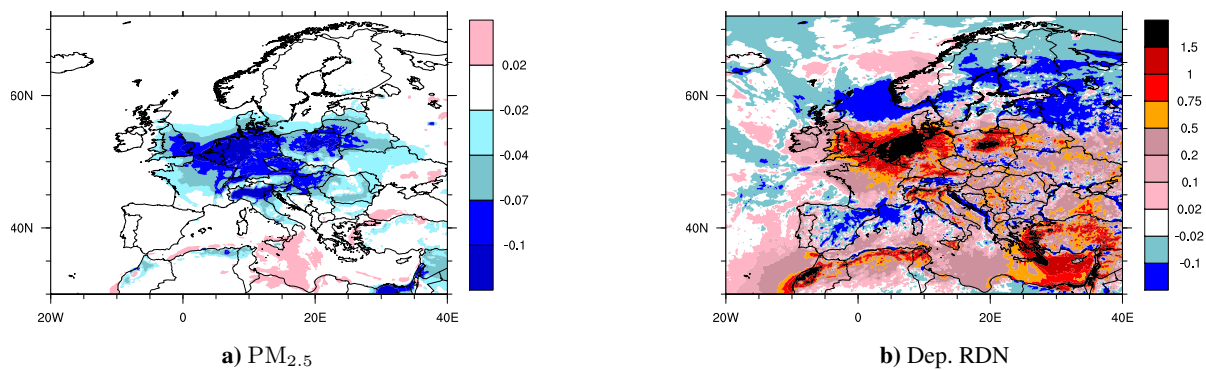

Figure 8. Difference between additional 50% – 40% reduction and additional Base–10% in NH$_3$ emissions on top of NEC 2030 for PM$_{2.5}$ concentrations [μgm^{-3}] (a), and deposition of reduced nitrogen [mg(N)m^{-2}] (b).

Appendix A

In this appendix we show scatter-plots of EMEP model results versus measurements for some key species for the years 2005 and 2017. Several of the 2017 scatter-plots have already been published in Gauss et al. (2019), but are shown here in order to provide a direct comparison to the year 2005 results. For year 2017 the comparison to measurements differ slightly from the results shown in Gauss et al. (2019) as several new measurements have been made available since the publication of the
470 above-mentioned report. For both years the scatter plots are shown with all measurements included. However, the selection of available measurements differs between the two years. In general there are more measurements available in 2017 compared to 2005. In Table A1 statistics for the scatter plots are listed for the same species as in the scatter plots, limiting the sites to those having measurements for both 2005 and 2017. The number of common measurements for both years are given in the table. In particular for NH_3 in air and HNO_3 in air there are very few sites with measurements for both years.

Table A1. Year 2005 and year 2017 statistics for scatter plots with common measurements sites for both years. Obs is observed annual meal for the sites include. Bias is model bias and Corr. is correlation between measurements and the model calculations.

Species	Nr. obs.	2005			2017		
		obs.	Bias	Corr.	obs.	Bias	Corr.
$PM_{2.5}$	14	11.34	-14%	0.57	7.75	-18%	0.84
NH_4^+ in air	13	0.94	-19%	0.94	0.57	-18%	0.89
NO_3^- in air	13	1.68	5%	0.71	1.44	-5%	0.80
NH_3 in air	7	0.76	26%	0.78	0.73	40%	0.90
HNO_3 in air	6	0.16	-12%	0.84	0.14	-33%	0.91

a) NH$_3$ in air (μg(N) m^{-3}) in 2005

b) NH$_3$ in air (μg(N) m^{-3}) in 2017

c) (NH$_4^+$) in air (μg(N) m^{-3}) in 2005

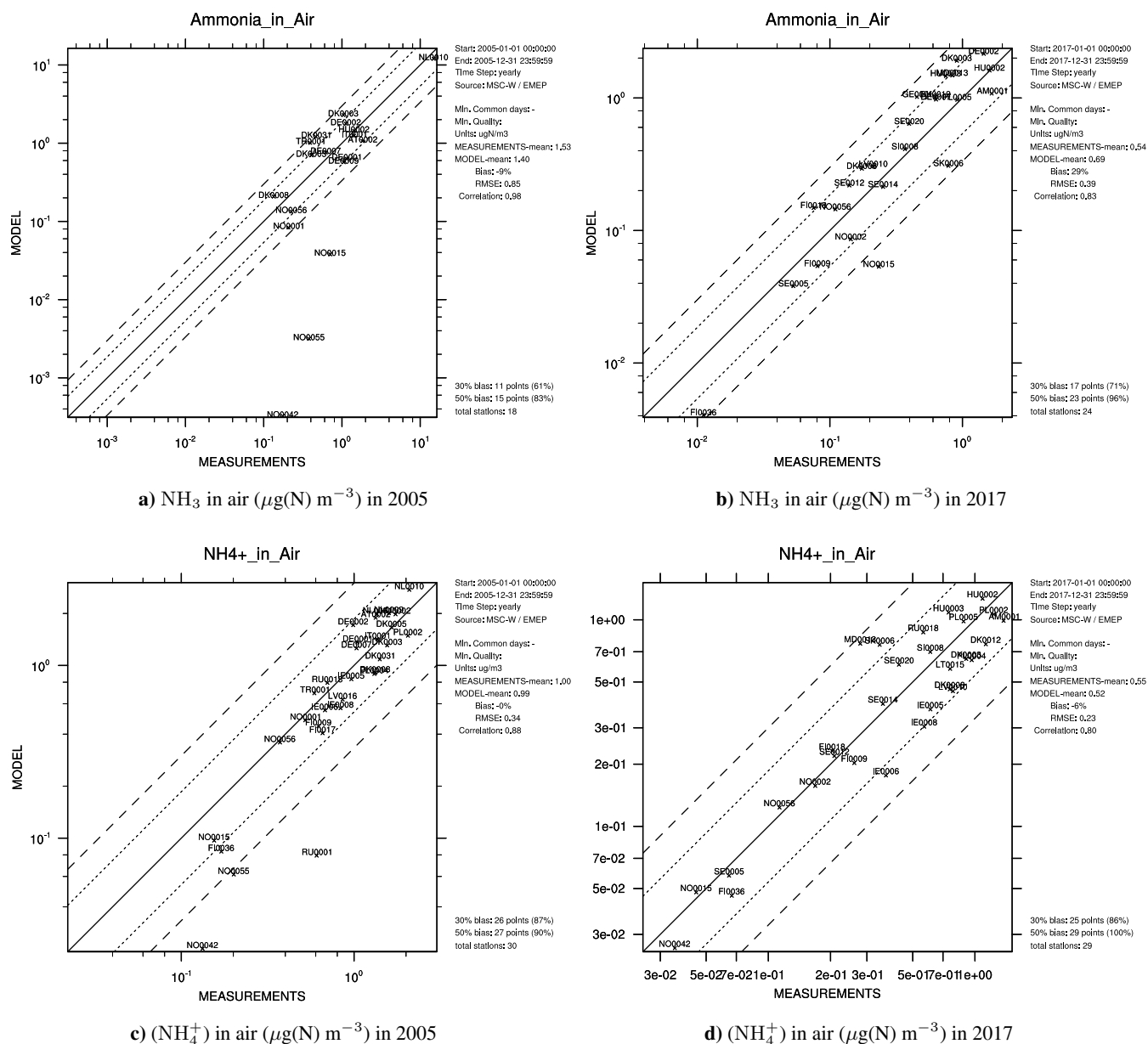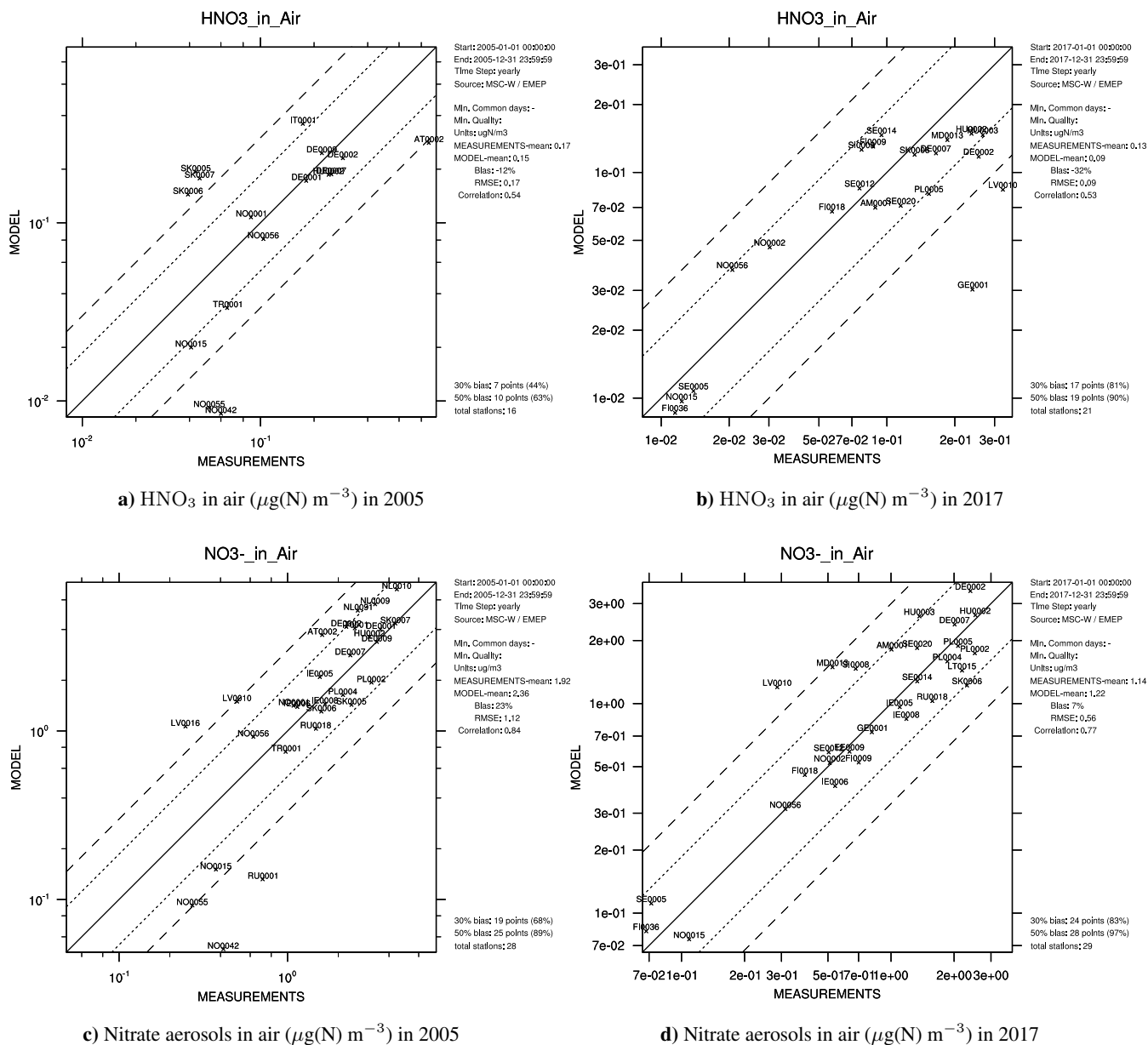**d)** (NH$_4^+$) in air (μg(N) m^{-3}) in 2017

Figure A1. Scatter plots of modelled versus observed concentrations of NH$_3$ (top) and ammonium (bottom) in air for the years 2005 (left) and 2017 (right). Statistics with limited set of common measurement sites are given in Table A1. Site positions listed in Tables A2 and A3. Measurements downloaded from http://ebas.nilu.no/default.aspx.

a) HNO_3 in air (μg(N) m^{-3}) in 2005

b) HNO_3 in air (μg(N) m^{-3}) in 2017

c) Nitrate aerosols in air (μg(N) m^{-3}) in 2005

**d)** Nitrate aerosols in air (μg(N) m^{-3}) in 2017

Figure A2. Scatter plots of modelled versus observed concentrations of nitric acid (top) and nitrate (bottom) in air for the years 2005 (left) and 2017 (right). Statistics with limited set of common measurement sites are given in Table A1. Site positions listed in Tables A2 and A3. Measurements downloaded from http://ebas.nilu.no/default.aspx.
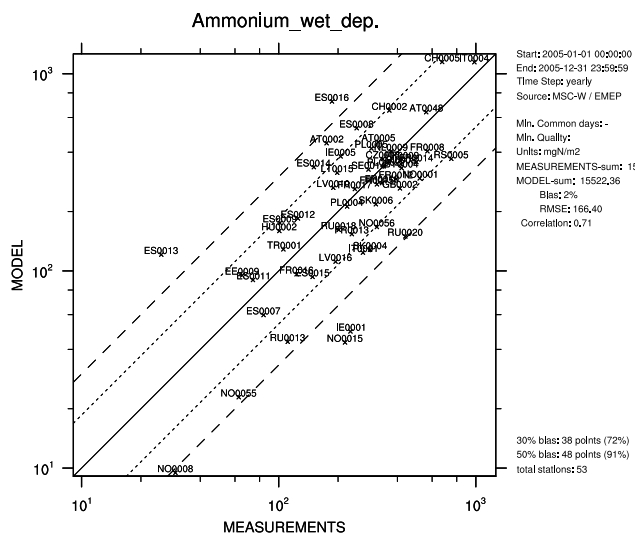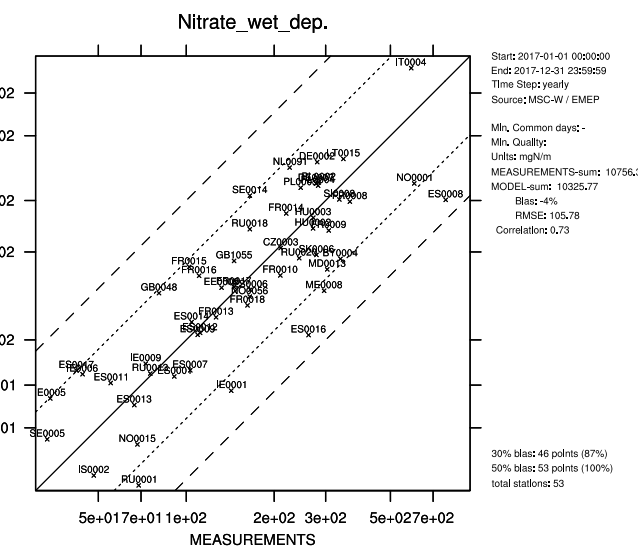
a) Wet deposition of reduced nitrogen (mg(N)m^{-2} in 2005
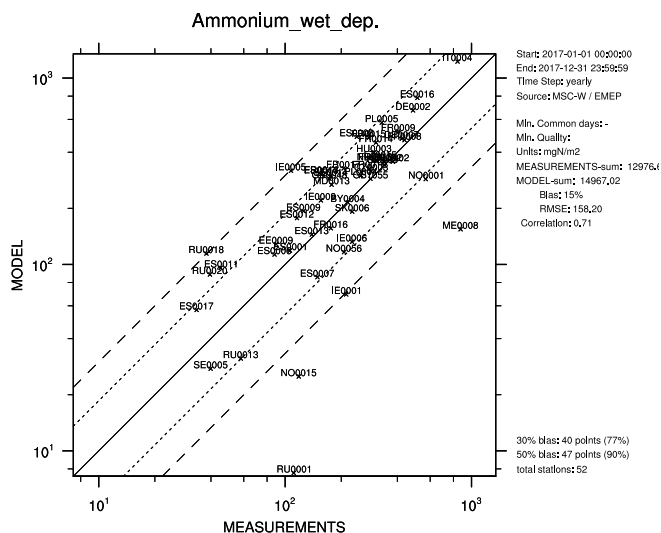
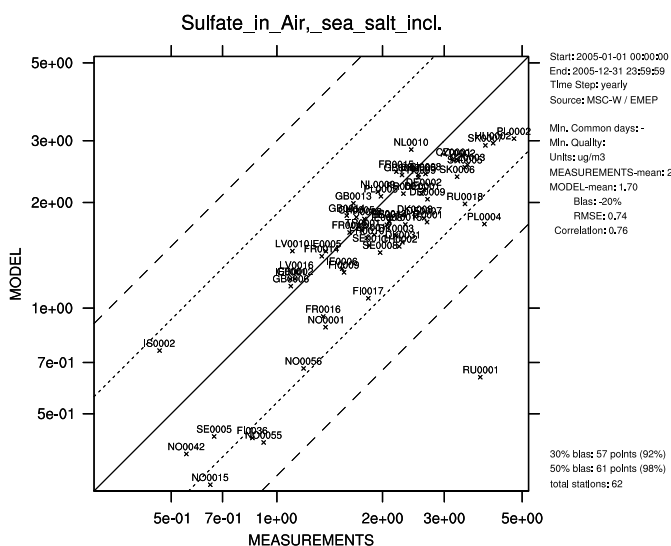**b)** wet deposition of reduced nitrogen (mg(N)m^{-2} in 2017
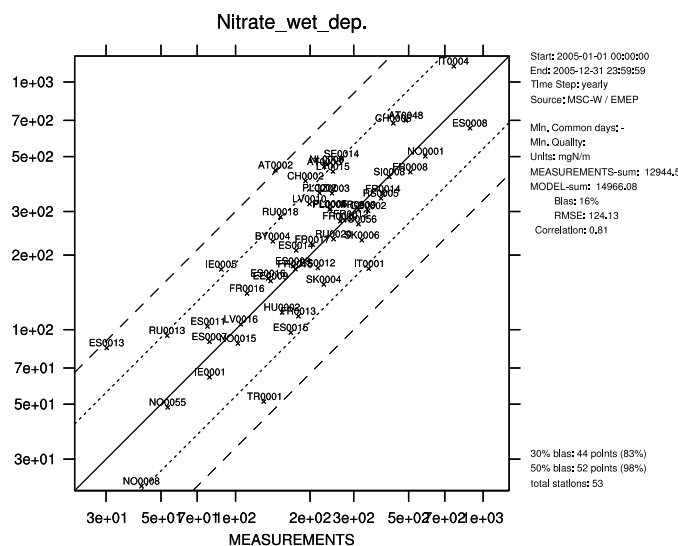
c) Wet deposition of oxidised nitrogen (mg(N)m^{-2} in 2005
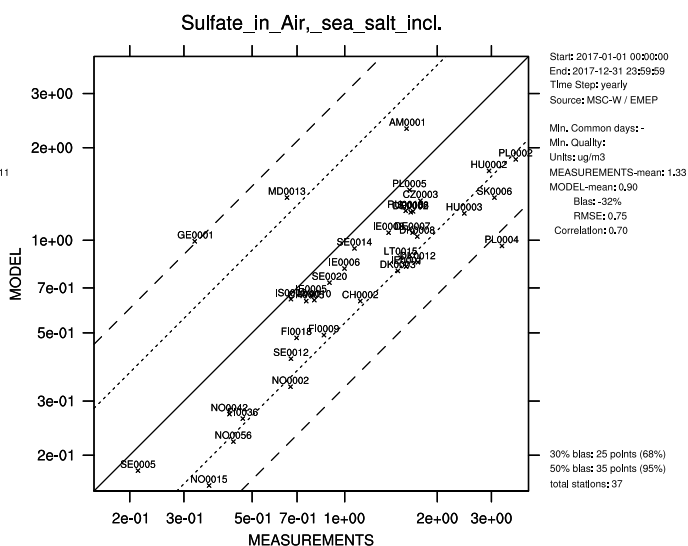
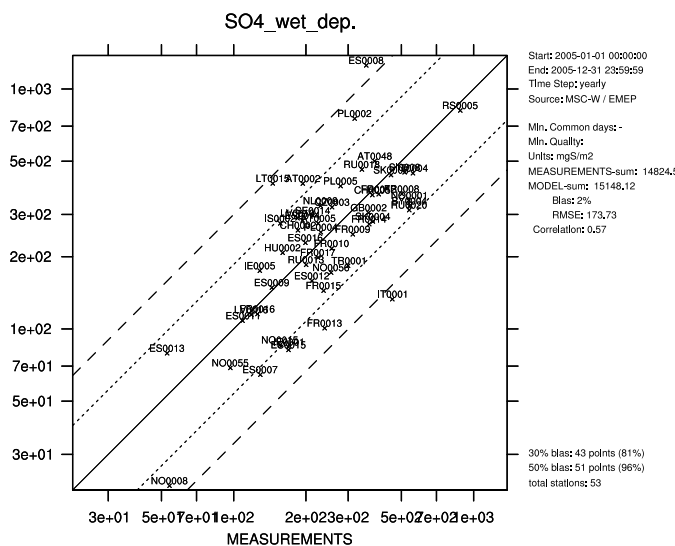**c)** Wet deposition of oxidised nitrogen (mg(N)m^{-2} in 2017

Figure A3. Scatter plots of modelled versus observed wet depositions of reduced nitrogen (top) and oxidised nitrogen (bottom) for the years 2005 (left) and 2017 (right). Statistics with limited set of common measurement sites are given in Table A1. Site positions listed in Tables A2 and A3. Measurements downloaded from http://ebas.nilu.no/default.aspx.

Sulfate_in_Air,_sea_salt_incl.

a) Sulphate in air (μg(S) m^{-3}) in 2005

Sulfate_in_Air,_sea_salt_incl.

d) Sulphate in air (μg(S) m^{-3}) in 2017

SO4_wet_dep.

c) Wet deposition of sulphate (mg(S)m^{-2} in 2005

SO4_wet_dep.

c) Wet deposition of sulphate (mg(S)m^{-2} in 2017

Figure A4. Scatter plots of modelled versus observed concentrations of sulphate in air (top) and wet deposition of sulphate (bottom) for the years 2005 (left) and 2017 (right). Statistics with limited set of common measurement sites are given in Table A1. Site positions listed in Tables A2 and A3. Measurements downloaded from http://ebas.nilu.no/default.aspx.
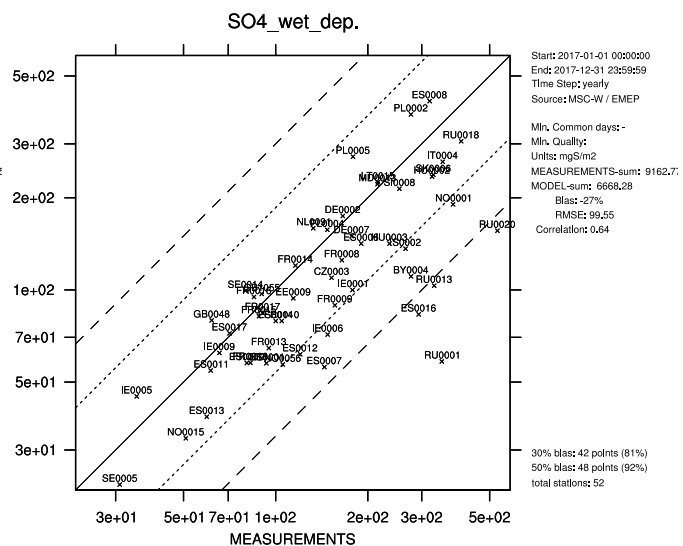
31

Table A2. List of sites included in scatter plots in Figures A1 to A4. Wet depositions when included for all three species (reduced nitrogen, oxidised nitrogen, and oxidised sulphur) marked with √. Only reduced and oxidised nitrogen marked with ∇, only oxidised N and S marked with △, only reduced N and oxidised S marked with ●, and only oxidised sulphur marked with ◊.

Site	Lat.	Lon.	NH$_3$		NH$_4^-$		HNO$_3$		NO$_3^-$		Wdep	
			2005	2017	2005	2017	2005	2017	2005	2017	2005	2017
IS0002	64.08	-21.02									◊	△
NO0001	58.38	8.25	√		√		√		√		√	√
NO0002	58.38	8.22		√		√		√		√		
NO0008	58.82	6.72									√	
NO0015	65.83	13.92	√	√	√	√	√	√	√	√	√	√
NO0042	78.91	11.89	√		√	√	√		√			
NO0055	64.47	25.22	√		√		√		√		√	
NO0056	60.37	11.08	√	√	√	√	√	√	√	√	√	
SE0005	63.85	15.33		√		√		√		√		√
SE0012	58.80	17.38		√		√		√		√		
SE0014	57.39	11.91		√		√		√		√	√	√
SE0020	56.04	13.15		√		√		√		√		
DK0003	56.35	9.60	√	√	√	√						
DK0005	54.75	10.74	√		√							
DK0008	56.70	11.52	√	√	√	√						
DK0012	55.69	12.09		√		√						
DK0031	56.30	8.43	√		√							
FI0009	59.78	21.38		√	√	√		√		√		
FI0017	60.52	27.69			√							
FI0018	60.53	27.67		√		√	√			√		
FI0036	68.00	24.24		√	√	√	√			√		
EE0009	59.50	25.90								√	∇	√
LV0010	56.16	21.17		√		√	√		√	√	√	
LV0016	57.14	25.91			√				√		√	
LT0015	55.37	21.03				√				√	√	√
RU0001	68.93	28.85			√				√			√
RU0013	64.70	43.40									√	√
RU0018	61.00	28.97			√	√			√	√	√	√
RU0020	56.53	32.94							√	√	√	√
BY0004	52.23	23.43									√	√
IE0001	51.94	-10.24									√	√
IE0005	52.87	-6.92			√	√			√	√	√	√
IE0006	55.38	-7.34			√	√			√	√		√
IE0008	52.18	-6.36			√	√			√	√		
IE0009	52.30	-6.51										√
GB0002	55.31	-3.20									√	
GB0048	55.79	-3.24										√
GB1055	51.15	-1.44										√
NL0009	68.00	24.24			√				√		√	√
NL0010	51.54	5.85	√		√				√			
NL0091	68.00	24.24			√				√			√
DE0001	54.93	8.31	√		√		√		√			
DE0002	52.80	10.76	√	√	√		√	√	√	√		√
DE0007	53.17	13.03	√	√	√		√	√	√	√		√
DE0009	54.44	12.72	√				√		√			

Table A3. See caption, Table A3

Site	Lat.	Lon.	NH$_3$		NH$_4^-$		HNO$_3$		NO$_3^-$		Wdep	
			2005	2017	2005	2017	2005	2017	2005	2017	2005	2017
PL0002	51.81	21.97			✓	✓			✓	✓	✓	✓
PL0004	54.75	17.53			✓	✓			✓	✓	✓	✓
PL0005	54.15	22.07		✓		✓		✓		✓	✓	✓
CZ0003	49.47	15.08									✓	✓
SK0004	49.15	20.28								✓	✓	
SK0005	49.37	19.68					✓		✓			
SK0006	49.05	22.67		✓		✓	✓	✓	✓	✓	✓	✓
SK0007	47.96	17.86					✓		✓			
CH0002	46.81	6.94									✓	
CH0005	47.07	8.46									✓	
AT0002	47.77	16.77	✓		✓		✓		✓		✓	
AT0005	46.48	12.97									✓	
AT0048	47.84	14.44									✓	
HU0002	46.97	19.58	✓	✓	✓	✓	✓	✓	✓	✓	✓	✓
HU0003	46.91	16.32		✓		✓		✓		✓		✓
MD0013	46.49	28.28		✓		✓		✓		✓		✓
ES0001	42.32	3.32										✓
ES0006	39.88	4.32										✓
ES0007	37.24	-3.53									✓	✓
ES0008	43.44	-4.85									✓	✓
ES0009	41.27	-3.14									✓	✓
ES0011	38.47	-6.92									✓	✓
ES0012	39.08	-1.10									✓	✓
ES0013	41.24	-5.90									✓	✓
ES0014	41.39	-0.73									✓	✓
ES0015	39.52	-4.35									✓	●
ES0016	42.63	-7.70									✓	✓
ES0017	37.05	-6.51										✓
FR0008	48.50	-7.13									✓	✓
FR0009	49.90	4.63									✓	✓
FR0010	47.27	4.08									✓	✓
FR0012	43.03	-1.08									✓	
FR0013	43.62	0.18									✓	✓
FR0014	47.30	6.83									✓	✓
FR0015	46.65	-0.75									✓	✓
FR0016	45.00	6.47									✓	✓
FR0017	45.80	2.07									✓	✓
FR0018	48.63	-0.45										✓
IT0001	42.10	12.63	✓		✓		✓		✓	✓	✓	
IT0004	45.80	8.63									✓	✓
SI0008	45.47	14.87		✓		✓		✓		✓	✓	✓
ME0008	43.15	19.13										●
RS0005	43.40	21.95									✓	
TR0001	40.00	33.00	✓		✓		✓		✓		✓	
GE0001	41.76	42.83		✓				✓		✓		
AM0001	40.38	44.26		✓		✓		✓		✓		